Hierarchy of abrupt transitions in the past climate

Denis-Didier Rousseau, Witold Bagniewski, Valerio Lucarini

Hierarchy of abrupt transitions in the past climate

Denis-Didier Rousseau (1,2,3), Witold Bagniewski (4)

(1) Université Montpellier, Géosciences Montpellier, Montpellier, France
(2) Silesian University of Technology, Institute of Physics-CSE, Division of Geochronology and Environmental Isotopes, Gliwice, Poland
(3) Columbia University, Lamont Doherty Earth Observatory, New York, USA
(4) Ecole Normale Supérieure – Paris Sciences et Lettres, Laboratoire de Météorologie Dynamique, Paris, France

Abstract (EGU2022 revised abstract)

The Earth's climate has experienced numerous abrupt and critical transitions during its long history. Such transitions are evidenced in accurate, high-resolution records covering different timescales. This type of evidence suggests the possibility of identifying and ranking past critical transitions, which yields a more complex perspective on climatic history. Such a context allows defining dynamical climate landscapes with multiscale features. To illustrate such a richer structure of critical abrupt transitions, we have analyzed 2 key high-resolution datasets: the CENOGRID marine compilation covering the past 66 Myr, and North Atlantic U1308 record representing the past 3.3 Myr. Our aim was to examine objectively the observed visual evidence of abrupt transitions and to identify among them, applying the augmented Kolmogorov-Smirnov test and the recurrence analysis, the key thresholds indicating regime changes that differentiate among major clusters of variability. This identification is replaced chronologically and discussed after comparison with major climate factors. A potential hierarchy in the observed thresholds is proposed through a domino-like succession of abrupt transitions, corresponding to as many bifurcations, that shaped the Earth's climate system over the past 66 Ma.

Introduction

Early evidence of abrupt transitions in Camp Century and Dye 3 Greenland ice cores (Dansgaard et al., 1969, 1982) attracted a lot of attention from the paleoclimatic community before being well acknowledged and understood. They have indeed introduced the evidence of a chain of abrupt climatic variations that at the time were unknown. Nonetheless, such transitions did not seem to find an agreement with other marine and terrestrial records, which led to considerable debate in the field (Broecker, 1975; Broecker et al., 1988; Broecker and Denton, 1989). After decades spent retrieving and studying much more detailed paleorecords, the evidence for such rapid climatic variations, named Dansgaard-oeschger events (DO), has been well accepted since then. They have been recently reinforced

by the identification of additional abrupt transitions from the NGRIP ice core, which have been made possible by the increased time-resolution of the record (Rasmussen et al., 2014). These additional events correspond to changes of either short duration or amplitude in $\delta^{18}O$ that visual inspection of or standard statistical inspections do not necessarily flag. Moreover, such new series of abrupt transitions have been described from marine (Bond et al., 1992) and continental (Wang et al., 2001) records, among other, providing a broader spatial perspective to that specific dynamical process for the climate system. Although interpreted as to be related to the last climate cycle, these abrupt transitions occurring in the last 130 kyr, have also been described in older records (Barker et al., 2011; Cheng et al., 2016; Rousseau et al., 2020), recent studies implying that DOs are likely to have existed since 0.9 Ma (Rousseau et al., 2022) or even earlier (Birner et al., 2016).

The Earth climate has experienced numerous abrupt and critical transitions during its long history (Hoffman et al., 2017; Scotese et al., 2021). Such transitions are evidenced in precise high-resolution records at different timescales. They have been interpreted as associated with abrupt climate changes, often corresponding to transitions, tipping points, leading to possibly irreversible changes in the state of the system. The study of tipping points has recently gained broad interest and perspective in Earth and Environmental sciences, especially with regard to the future of our societies under the present climate warming scenarios (Lenton et al., 2008; Lenton, 2013; Lenton et al., 2019; Brovkin et al., 2021). The term Tipping Elements (TE) was introduced by Lenton and Williams (2013), Lenton et al. (2019), and subsequently adopted by others (Lenton, 2013; Steffen et al., 2018) to characterize the particular components of the Earth System that are likely to experience a tipping point (anticipated TPs) in a near future. These TEs relate to all the components of the Earth system: the atmosphere, the cryosphere, the ocean, the land surface and the biosphere, and are more or less interconnected (Kriegler et al., 2009; Brovkin et al., 2021; Wunderling et al., 2021). More recently tipping point concept starts being applied to socio-economical features (Otto et al., 2020; Lenton et al., 2022).

To illustrate such an idea, we have analyzed 2 key high-resolution datasets of the past 66 Myr and showing evidences of abrupt transitions. The first time series is the CENOGRID benthic $\delta^{18}O$ and $\delta^{13}C$ corresponding to the compilation of 14 marine records over the past 66 Myr (Westerhold et al., 2020). The second corresponds to the North Atlantic U1308 benthic $\delta^{18}O$, $\delta^{13}C$ and δ^{18}bulk carbonate records covering the past 3.3 Myr (Hodell and Channell, 2016). The aim was to examine the observed visual evidences of abrupt transitions and to identify among them key abrupt thresholds by applying the Kolmogorov-Smirnov (KS) test and the recurrence quantification analysis (RQA) (Bagniewski et al., (2021),-see methods). In a second step, the selected transitions are discussed and replaced in the Earth climate history allowing the definition of dynamical succession of abrupt transitions. In a third step, we replace the potential succession of abrupt transitions in time series of key climate factors such as CO2 concentration, average global sea level, and depth of the carbonate compensation. The forth step

searches for the presence of a nontrivial structure for the recurrence plot that would be indeed indicative of the multiscale nature of the quasi-potential of the benthic $\delta^{18}O$ and $\delta^{13}C$. This leads to conclude by proposing a potential hierarchy in the observed thresholds, and the definition of a domino-like succession of abrupt transitions that shaped the Earth climate system over the past 66 Ma.

Results

The KS augmented test of the benthic $\delta^{18}O$ record of the past 66 Ma identifies six major abrupt transitions corresponding to two major warming events at about 58Ma and 56Ma, followed by four major coolings at 47Ma, 34Ma, 14Ma and 2.9 Ma respectively (Fig. 1a). These events are classical ones described from the literature (Zachos et al., 2001), where the first two transitions led to warmer conditions, while the latter four led to colder conditions. The recurrence plot (RP) and recurrence rate (RR) analyses of the same dataset identify also these major transitions, with a few more –like at 63Ma, 40Ma and 9.7Ma (Fig. 1c, Suppl. Tab. 1). We have chronologically labeled these TP1 to TP9. All these abrupt events are associated with clusters at different scales in the RPs, and, in particular are separated into two different macroclusters prior and after 34 Ma, the well-known Eocene-Oligocene Transition (EOT) (Zachos et al., 1992). Such pattern characterizes two different types of variability regimes illustrating two types of state of the Earth Climate System (see Fig. 1b).

The older macrocluster shows a disrupted variability, according to Marvan nomenclature (2007), bounded by the abrupt transitions identified at 66 Ma and 34 Ma respectively. Such particular distribution corresponds to a response of the Earth system to some particular forcings to be determined later in the study. The main features of the oldest cluster are the most negative values of the benthic $\delta^{18}O$ corresponding to the very warm climate conditions that were prevailing between 66 Ma and 34 Ma. The average global temperature was estimated to be between 8°C and 16°C above the present day one (Westerhold et al., 2020) (Fig. 1a). No evidence of the presence of any major continental ice bodies is recorded by the $\delta^{18}O$ values. However with this warm period further, hierarchically yet relevant abrupt transitions are found, including 2 major abrupt warmings at 58 Ma (TP2) and 56 Ma (TP3) respectively detected by both methods. These two transitions correspond to thresholds towards much warmer oceanic deep water corresponding to the first late Paleocene-Eocene hyperthermal (Thomas et al., 1999; Miller et al., 2020) and Paleocene-Eocene Thermal Maximum (PETM) (Kennett and Stott, 1991; Dickens et al., 1997) respectively. The third one at about 47 Ma (TP4) corresponds to a transition towards cooler deep waters and named the Early-Middle Eocene cooling (Miller et al., 2020).

The more recent macrocluster presents, on the contrary, a different pattern indicating a repetition of sub-clusters showing a drifting variability from 34 Ma onward, characterizing non-stationary systems with slowly varying parameters. This second state characterizes colder climate conditions prevailing

from 34 Ma to present day. This cold climate macrocluster is characterized by more positive values of benthic $d^{18}O$ and shows about 20 Myr of mostly stationary climate until 14 Myr (TP7) (Kennett and Shackleton, 1976; Shackleton, 1985). Three abrupt transitions during the last 14 Myr, are associated, in the recurrence plot, to the presence of four recurrent patterns occurring at consecutive times: from 34 Ma (TP6) to 14 Ma (TP7), from 14 Ma to 9.7 Ma (TP8), from 9.7 Ma to 2.9 Ma (TP9), and from 2.9 Ma to present. These may be rather related to some internal factors of the Earth climate system, as described for more recent timescales (Bagniewski et al., 2021; Rousseau et al., 2022).

Such general pattern of the RP for the 66 Myr translates an apparent irreversibility of the climate responses at 34 Ma (TP6), a date that must be therefore interpreted as a major threshold, a hierarchically dominant tipping point associated with the transition between two fundamentally different modes of operation of the climate system, represented by the two macro clusters.

Contrary to the benthic $\delta^{18}O$, the $\delta^{13}C$ RP shows a different pattern. Benthic $\delta^{13}C$ values rather characterize deep water ventilation with high $\delta^{13}C$ values in regions close to deep water formation area. The recurrence plot and recurrence rate analyses of the benthic $\delta^{13}C$ record yield 10 abrupt transitions among which three at 56.15 Ma, 34 Ma, and 7.15 Ma on the contrary respectively appear more important (SuppFig. 1, Suppl. Tab. 1). The interval 56.15 Ma – 7.15 Ma is well individualized showing some subclusters distributed around 34 Ma, which is identified, once more, as a key threshold. The 56.15 Ma date groups $\delta^{13}C$ values above 1‰, at the base of the record, while 7.15 Ma gathers the negative $\delta^{13}C$ values which mainly occurs on top of the record. These intervals are themselves characterized by two very different and opposed climate conditions with regards to a reference state represented by the 56.15 Ma – 7.15 Ma interval. The upper climate regime translates more addition of carbon in the ocean while the lower cluster rather characterizes more addition of carbon in the atmosphere. These different thresholds are also identified by the KS test, which nevertheless detects some more at about 54.5 Ma, 37.5 Ma, and 16 Ma. A last threshold is identified with two different dates according to the method applied: 22 Ma from the KS test and 23 Ma from RP analysis.

The past 3.3 Ma record from North Atlantic core U1308, can be considered as a blow up of the CENOGRID dataset over this particular time interval (Fig. 2). The variations in the deep-water temperature, as expressed by the benthic $\delta^{18}O$, are also interpreted as an indicator of the continental ice volume with clear interglacial-glacial successions (Chappell and Shackleton, 1986; Shackleton, 2000; Elderfield et al., 2012). The KS augmented test of the benthic $\delta^{18}O$ allows identifying the classical transitions characterizing the Marine Isotope Stages (MIS) as already observed in numerous records covering that interval (see Rousseau et al. (2022) and herein). Such observation illustrates the clear response, during this interval, of the Earth Climate system to the classical external forcings (mostly obliquity at the base and eccentricity on top of the record) expressed in the astronomical theory of climate (Milankovic, 1920,

1941; Hodell and Channell, 2016). The critical transition of the Mid-Pleistocene (MPT), between 1.25Ma and 0.8Ma, is well evidenced. The RP and RR of the benthic $\delta^{18}O$ record of U1308 indicate a drifting regime. This pattern appears similar to that already identified in the youngest macrocluster, for the recent 34Myr, determined also from the benthic $\delta^{18}O$ CENOGRID record. In U1308, it individualizes particular abrupt transitions responses at 2.93 Ma, 2.52 Ma, 1.51 Ma, 1.25 Ma, 0.61 Ma, and 0.35 Ma respectively (see Fig. 2b,c, Suppl. Tab. 1 - Rousseau et al. (2022)). As they transition with the CENOGRID record, the abrupt thresholds at 2.93 Ma and 2.52 Ma have been labeled TP9 and TP10. On the contrary, the youngest transitions are interpreted as critical transitions and labeled CT1 (1.5 Ma) to CT4 (0.35 Ma) (Fig. 2)

Contrary to the CENOGRID $\delta^{13}C$ RP, U1308 $\delta^{13}C$ RP shows a drifting pattern similar to that of benthic $\delta^{18}O$, with only 2 key transitions at 2.52 Ma and 0.48 Ma (see Suppl. Fig. 3). However, beside the 2.52 Ma date, the 0.48 Ma does not have any equivalent in the benthic $\delta^{18}O$ records.

A complementary RQA of the $\delta^{18}O$ bulk carbonate record from U1308, which characterizes episodes of iceberg calving into the North Atlantic Ocean, and therefore illustrates the dynamics of the Northern Hemisphere ice sheets (NHIS), yields almost similar dates than those obtained for the benthic $\delta^{18}O$ record (see Suppl. Fig. 3, Suppl. Tab. 1) (Rousseau et al., 2022). Finally, when zooming over the last 0.7 Ma of U1308 benthic $\delta^{18}O$ record, the RP shows a particular pattern of periodicity, with the last 0.65 Ma differentiated into 3 sub-clusters before the present interglacial (0.10 Ma), bounded respectively at 0.61 Ma, 0.43 Ma, 0.35 Ma and about 0.15 Ma.

Interpretation, discussion

Replacing the different dates identified by the KS test and RQA from our two key records on a chronological perspective, the determined transitions appear in a particular order, with the threshold at 34Ma, corresponding to Eocene-Oligocene Transition (EOT), being central in the Cenozoic climate history. Indeed, after 66 Ma, the Earth is highly recovering from the intense reset provoked by the Chicxulub Meteorit impact (Gulick et al., 2008, 2013, 2017, 2019) affecting both the Earth's climate and biodiversity as indicated through three different factors that are discussed below.

1 The Past 66Myr – 3 Myr history of the Earth Climate

Using benthic foram $\delta^{18}O$ and Mg/Ca records from high-resolution Pacific cores different from CENOGRID ones, Miller et al. (2020) have reconstructed the variations of the global mean sea level (GMSL) of the past 66 Ma. GMSL has strongly impacted the global oceanic circulation, and determined the extent of the emerged and inundated land areas, especially the continental shelves allowing or preventing, associated to plate tectonics, continental biological migrations. Measuring the carbonate

content in sediment Pacific cores and applying transfer functions, Pälikhe et al. (2012) have computed a detailed Cenozoic record of the Pacific carbonate compensation depth (CCD) below which carbonates dissolve. CCD represents therefore an indicator of the ocean carbonate saturation state and is linked to the atmospheric CO_2 concentration present above the sea surface. Finally, compiling estimates from various proxies including foram $\delta^{13}C$, boron isotopes, stomata, paleosols… Beerling and Royer (2011) have released a comprehensive Cenozoic record of the CO_2 concentration that shows a large variability especially for the older interval, due to greater uncertainties in the reconstructions. We have thus replaced the major thresholds (TP) detected in our KS test and RQA against the GMSL, CCD, and CO_2 time series to interpret our results (Fig. 3).

One first notices that TP6 major transition at 34 Ma (EOT) is observed once more in the three factors, corresponding to an abrupt lowering of the GMSL of about 70m, of the CCD of around 1000m, of the CO_2 concentration, which are considerable changes (Fig. 3). TP6 splits these three time series into the same two main intervals than those previously observed from the RQA of the CENOGRID benthic $\delta^{18}O$ and $\delta^{13}C$ records. Such result suggests therefore that correspondences may exist between these factors and the two parameters (Figs. 1,3, Suppl. Tab. 2), which differed prior and after EOT. An evident variability appears in the responses of the climate to various mechanisms, under four identified states, from "Warmhouse" (66Ma-TP2 and TP4-TP6) and "Hothouse" (TP2-TP4) climates, to "Coolhouse" (TP6-TP7) and "Icehouse" climates (TP7 to present); (see Fig. 1),

The first two states alternated, from 66 Ma until 34 Ma, in a warm-hot-warm sequence under extremely high CO_2 concentrations (Beerling and Royer, 2011) compare to those measured over the past 800 kyr in the Antarctic ice cores, which represent the reference states for the IPCC potential scenarios of climate change warming (IPCC, 2021) (Fig. 3c). This first main interval shows the highest values of the Cenozoic era in GMSL, CO_2 concentration and CCD depth whose average values are: +38.47 ± 14.85m, 626.96 ± 311.79 ppmv and 4586 ± 153.01 m respectively (Suppl. Tab. 2). Conversely, the last two states succeeded each other, from 34 Ma onward present time, under much lower CO_2 concentrations and GMSL, thus generating the classical climate trend towards the recent ice-age conditions (Zachos et al., 2001; Westerhold et al., 2020; Scotese et al., 2021) (Fig. 3a,c). Indeed the last 34 Myr show average values in GMSL, CO_2 concentration and CCD depth of -3.49 ± 12.90 m, 329.89 ± 164.47 ppmv and 3518.67 ± 408.92 m respectively (Tab. 2), which are much lower than in the older interval. This second set of means are underestimated values because the final values of Miller et al. (2020) dataset ending at 0.9Ma,

These GMSL, CCD and CO_2 reconstructions shows key transitions that fit with the CENOGRID thresholds deduced from the KS and RR analysis of the benthic $\delta^{18}O$ although they characterize either an increase or a decrease in the global mean sea level corresponding roughly to warming or cooling episodes of the Earth history or strong variations in the concentration of atmospheric CO_2. The variations observed in

CO_2, CCD and GMSL, at the 10 identified TPs from the benthic $\delta^{18}O$ record, indicate inhomogeneous characteristics prior TP6 major threshold (Suppl. Tab. 3). On the contrary homogenous trends are noticed in the three climate proxies after TP6, translating the occurrence of major reorganizations in the climate system, which become interesting to test at a shorter timescale.

Studying the same CENOGRID dataset, Boettner et al. (2021) identified 9 geological transitions at respectively 62.1 Ma, 55.9 Ma, 33.9 Ma, 23.2 Ma, 13.8 Ma, 10.8 Ma and 7.6 Ma, the latter mainly from the $\delta^{13}C$ record. Four of them are indeed identical to those determined in the present study: 62.1 Ma, 55.9 Ma, 33.9 Ma and 13.8 Ma, the first two being preceded by a significant early warning signal (Boettner et al., 2021) which does not appear to be the case for the EOT key transition..

2 The Past 3.2 Myr history of the Earth climate, mainly from Northern Hemisphere

As indicated previously, the last 3.3 Myr have been defined as an Icehouse climate state, with the appearance of NHIS, their development and variations through time (Westerhold et al., 2020) while Antarctic ice sheets already reached mostly their maximal expansion. This Icehouse state is characterized by a change of the interplay between benthic $\delta^{13}C$ and $\delta^{18}O$, which corresponds to a new relationship between the carbon cycle and climate (Turner, 2014).

The RQA of U1308 benthic foram $\delta^{18}O$, we have identified six steps in the $\delta^{18}O$ variability (Fig. 2, Suppl. Tab. 1). They correspond to abrupt transitions dated at 2.95 Ma, at 2.55 Ma, at 1.5 Ma, at 1.25 Ma, at 0.65 Ma and at 0.35 Ma, which characterize the dynamics of North Hemisphere ice sheets (elevation and spatial expansion). Interestingly, the interval 1.25 Ma to 0.65 Ma corresponds roughly to the previously mentioned MPT, during which a shift occurred from climate cycles dominated by a 40-kyr periodicity to 100-kyr dominated ones (Shackleton and Opdyke, 1977; Pisias and Moore, 1981; Ruddiman et al., 1989; Clark and Pollard, 1998; Clark et al., 2006). The 1.25 Ma date is particularly significant, since it is followed by an increase in the amplitude of glacial–interglacial fluctuations. The $\delta^{18}O$ bulk carbonate record in the U1308 core, in turn, is interpreted as characterizing IRD released into the North Atlantic Ocean (Hodell and Channell, 2016). The RQA of this record also displays a drifting regime, and it yields abrupt transitions at 2.75 Ma, at 1.5 Ma, at 1.25 Ma, at 0.9 Ma and 0.65 Ma which characterize the dynamics of NHIS through episodic to more regular and of larger magnitude iceberg calving (Supp. Fig. 2)

These abrupt transitions identified during the past 3.2 Myr occur in the Earth context where the Antarctic ice sheets are built and had already a major impact on the course of the Earth climate. Although significant, they relate to the evolution of NHIS history and therefore could be rather labeled Critical Thresholds (CT) (see Fig.).

A hierarchy of abrupt transitions

Traditionally, tipping points are schematically represented as being associated with the bifurcation occurring for a system described by a one-dimensional effective potential when a change in the value of a certain parameter leads to a change in the number of stable equilibria. Hence, conditions describing the nearing of a tipping point can be related to the presence of slower decay of correlations (critical slowing down). This viewpoint, while attractive, suffers from many mathematical issues due to the fact that the true dynamics of the system occurs in a possibly very high dimensional space. Tantet et al. (2018a,b) have introduced a mathematically rigorous framework for the occurrence of tipping points that clarifies the link between rate of decay of correlations, sensitivity of the system to perturbations, and robustness of the unperturbed dynamics.

This suggests the possibility at identifying a potential hierarchy of past critical events, which would give a more complex perspective on the history of the climate than the classical saddle-node two-dimension representation of tipping points described above. Indeed, Lucarini & Bodai (2019, 2020) proposed to describe the global properties of the climate system using the formalism of the Graham (1987) quasi-potential. The minima of such quasi-potential, which has strong similarities with the epigenetic landscape of Waddington (1942), correspond to local maxima of the probability distribution of the system associated with the competing climatic states, and the saddles correspond to the Melancholia states (Lucarini and Bodai 2017) of the system, gateways for the noise-induced transitions between such states. Margazoglou et al. (2021) suggested that the presence of decorations of the quasi-potential at different scales would lead exactly to a hierarchy of tipping points (Fig. 4: YOUR FIGURE OF QUASI-POTENTIAL HERE?)

Added to the Chicxulub meteor impact previously mentioned, which injected a considerable amount of CO_2 into the atmosphere (O'Keefe and Ahrens, 1989; Lomax et al., 2001), Deccan traps were already spreading at the beginning of the Cenozoic, contributing to the release of massive amount of CO_2 (Scotese et al., 2021). CO_2 concentration continued raising until about 500 ppmv with the North Atlantic Igneous province very active at about 58 Ma - 56Ma (TP2 and TP3) in relation with the opening of the North Atlantic Ocean (Jolley and Bell, 2002). The Northern Hemisphere plates were connected and not facing the present Arctic conditions allowing faunal and vegetal dispersion. Other plates were on the contrary reorganizing like India moving northeastward toward the Asian continent. Equatorial Pacific carbonate compensation depth (CCD) reached a minimum value a bit later at about 54 Ma when CO_2 concentration reached its maximum of the whole Cenozoic above 1,100 ppmv (Beerling and Royer, 2011). The lowering of the GMSL and of the CCD at TP4 (about 40 Myr) has been interpreted as the start of the icing of Antarctica through mountain glaciers deposits dates by K-Ar dating of lava flows (Birkenmajer et al., 2005), supported by other glacial evidences i.e., from the Gamburtsev subglacial mountains (Rose et al.,

2013), while Northern Hemisphere plates remained connected. By TP4 India is approaching the Asian plate while Northern Hemisphere ones were still connected, allowing northern continental migrations of mammals at high latitudes (Janis, 1993; Torsvik and Cocks, 2016). At TP6, about 34 Myr, the Drake and Tasmanian passages are opening (Lagabrielle et al., 2009), even if several steps, inducing a drastic change in the whole deep and surficial oceanic circulation, characterized by a decrease in the South Hemisphere water formation strength, a deep sea temperature drop associated with the deep fall in relative sea level and CCD (see Fig. 3). According to paleoaltimetry estimates based on oxygen isotopes, Rowley and Currie (2006) indicate that the Tibetan Plateau had an elevation of about 4000m, favoring therefore the physical weathering of rocks, consuming CO_2, and the burial of carbon through high sedimentation rates in the adjacent seas. This may have contributed to the major threshold in the variation of the CO_2 concentration, which also drops very strongly (Beerling and Royer, 2011; Fig. 3).

This key transition is the major boundary between two different climate landscapes dominated by intensive plate tectonic and major volcanism for the older one, and by major ice sheets in both Southern and Northern Hemispheres, with plate tectonic (closure of seaways, orogenies) still very active, for the younger one (Torsvik and Cocks, 2016). Immediately after the EOT, the climate witnessed the build up of the East Antarctic ice sheet (Oi-1 glaciation), which can be considered as the onset of the cold world in which we are still living. India has almost ended its transfer to the Asian plate. Between TP6 and TP 7, i.e., 34 and 14 Myr respectively, the East Antarctic ice sheet is waxing and vaning with several major glaciations occurring before the 17 Myr to 14.5 Myr interval during which sea level increases in association with a severe shoaling episode of CCD and higher values of the CO_2 concentration (Fig. 3). Such high CO_2 concentrations may have been fueled by the Columbia River major volcanism, which ended by TP 7 at about 14 Ma (Scotese et al., 2021). Plate tectonics is still very active with the closure of both the Indonesian gateway and the Tethyan seaway, contributing to the start of the development of the Mediterranean (Bialik et al., 2019), and. Eurasia is now separated from Northern America and Greenland, India colliding the Asian continent, and the Andes are uplifting modifying the geometry of the marine basins and the global oceanic circulation. West Antarctica is starting building up while East Antarctic ice sheet is reinforcing and expanding. TP8 at about 9 Ma sees a strong lowering of the GMSL and of the CO_2 concentrations (Fig. 3). The final major tectonic event corresponds to the closure of the Panama Isthmus at TP9, which definitively configure the oceanic circulation close to the current one (Lunt et al., 2008). This is associated to a strong lowering of the global sea level, a deepening of the CCD and the CO_2 concentration (Fig. 3) that will preside the Earth climate history during the Quaternary, associated to the build up of the Northern Hemisphere glaciers and ice sheets. It is interesting to notice that all the major transitions that have been identified during the interval between 66 Ma and 2.9-2.5 Ma, are linked to the build up, waxing and vaning of the Northern and Southern Hemisphere ice sheets.

Considering the results of both RQA, KS test and quasi-potential view point, a concept of a hierarchy of abrupt transitions can therefore be proposed as described in figure 5, showing the major climate transitions, TP1 to TP10, which shaped the Earth climate towards the onset and development of the Southern ice sheets and the later build up of the NHIS, impacted by critical thresholds (CT1 to CT4) which steered their development and evolution. Such evolution occurred within two different climate landscapes bounded by the 34 Ma major transition. Without the major drop in GMSL, in CO2 concentration and in CCD, the Earth climate could have been different. However passing this major threshold, the Earth climate entered a new landscape marked by much lower CO2 concentration, lower GMSL and CCD. The oceanic basin redesign and the mountain uplifts changed the marine and atmospheric circulations patterns, leading to the onset and development of the NHIS. Variations in these NHIS extent and volume have contributed to the occurrence of the millennial variability marked by the Bond cycles as better described during the last climate cycle but, which onset has been proposed to be dated of 0.9 Ma (Rousseau et al., 2022). This succession of abrupt transitions characterizes a domino-like effect leading the Earth System to pass from one climate landscape to another under the natural regulation of the astronomical parameters. However, a new and unexpected future abrupt transition has to be considered with high confidence as noticed by instrumental observations impacting numerous tipping elements (see Lenton, 2013) through very drastic tipping cascades (Brovkin et al., 2021). This potential upcoming major transition does not seem to follow the previous succession of CT observed during the past 2.9 Myr and maintaining the climate variability within the same climate landscape. This potential major transition rather could be the boundary between the Cenozoic icehouse tipping landscape and another new one corresponding to the strong variations in key climate factors induced by the human activity. Indeed, IPCC reports and other published evidences are demonstrating that both climate and biodiversity seem evolving towards possible irreversible changes, making this upcoming abrupt transition a major tipping point in the Earth System, similar to TP6 at 34 Ma, involving perhaps new parameters to be considered, but also leading to a new and unknown climate landscape (Fig. 5)

Methods

The augmented Kolmogorov-Smirnov test is a robust method for finding local maxima and minima in a particular time series and is therefore a very precise way for timing the onset of abrupt transitions successfully applied to various geological time series. The method compares two samples taken before and after the potential transition point to test whether they come from the same continuous distribution. If they do not, the transition point is identified as a significant abrupt change indicative of a true climatic shift. (see for more details Bagniewski et al., 2021; Rousseau et al., 2022)

To gain further insight like recurring patterns into the climate story the records tell us, we performed a quantitative, objective analysis of these time series of proxy variables, based on the recurrence plots (RPs) introduced by Eckmann et al. (1987) into the study of dynamical systems and popularized in the climate sciences by Marwan et al. (2007, 2013). The RP for a time series $\{x_i : i = 1, \ldots, N\}$ is constructed as a square matrix in a cartesian plane with the abscissa and ordinate both corresponding to a time-like axis, with one copy $\{x_i\}$ of the series on the abscissa and another copy $\{x_j\}$ on the ordinate. A dot is entered into a position (i, j) of the matrix when x_j is sufficiently close to x_i. For the details — such as how "sufficiently close" is determined — we refer to Eckmann et al. (1987) and to Marwan et al. (2013). All the points on the diagonal $i = j$ have dots and, in general, the matrix is rather symmetric, although one does not always define closeness symmetrically; to wit, x_j may be "closer to" x_i than x_i is to x_j (Eckmann et al., 1987). An important advantage of the RP method is that it does apply to dynamical systems that are not autonomous, i.e., that may be subject to time-dependent forcing. The latter is certainly the case for the climate system on time scales of 10–100 kyr and longer, which is affected strongly by orbital forcing.

Eckmann et al. (1987) distinguished between large-scale *typology* and small-scale *texture* in the interpretation of square matrix of dots that is the visual result of RP. Thus, if all the characteristic times of an autonomous dynamical system are short compared to the length of the time series, the RP's typology will be homogeneous and, thus, not very interesting. In the presence of an imposed drift, a more interesting typology will appear. The most interesting typology in RP applications so far is associated with recurrent patterns that are not exactly periodic but only nearly so. Hence, such patterns are not that easily detectable by purely spectral approaches to time series analysis. Marwan et al. (2013) discuss how to render the purely visual RP typologies studied up to that point more objectively quantifiable by recurrence quantification analysis and bootstrapping (Efron, 1981; Efron and Tibshirani, 1986). The RP exhibits, moreover, a characteristic texture — given by the pattern of vertical and horizontal lines that mark recurrences. These lines sometimes form recurrence clusters that correspond to specific periodic patterns.

The quasi-potential analysis…

Figure captions:

Fig. 1. **KS test and Recurrence Quantitative Analysis (RQA) of CENOGRID benthic $\delta^{18}O$.** a) Time series in Ma BP with difference of the reconstructed and present Mean Global Temperature in pink). KS test identifying abrupt transitions towards warmer conditions in red and cooler or colder conditions in blue; b) Recurrence plot (RP) with identification of the main two clusters prior and after 34 Ma. The main abrupt transitions identified are highlighted by red circles, and c) Recurrence rate (RR). The pink crosses and vertical green lines indicate the abrupt transitions (TP) detected by the RQA. CENOGRID benthic $\delta^{18}O$ data are from Westerhold et al. (2020)

Fig. 2. **RQA of U1308 benthic $\delta^{18}O$**. a) Time series in Ma; b) RP; and c) RR. Crosses similar than Fig. S1. TP9-10 and CT1-4 abrupt transitions identified in the RR. U1308 benthic $\delta^{18}O$ data are from Hodell and Channell (2016)

Fig. S3; **Variation through time of three main climate factors and comparison with the identified abrupt transitions (TP) in the CENOGRID benthic $\delta^{18}O$.** a) Global Mean Sea Level in meters from Miller et al, (2020). Identification of particular warm intervals and glaciation events. The Laurentide, GIW-WAIS and Ice free lines are from Miller et al. (2020); b) Carbonate Compensation Depth (CCD) in meters from Palike et al., (2012). The purple circles identify the TPs on this record; c) Estimate of the CO_2 concentration in parts per million volume (ppmv) from Beerling and Royer (2011). The Antarctica glaciation threshold at 750 ppmv and the NH glaciation threshold at 280 ppmv lines respectively are from De Conto et al. (2008).

Fig. 4. **Quasipotential plot of CENOGRID benthic $\delta^{18}O$ and $\delta^{13}C$.**

Fig. 5. **Evolution of the Earth Climate history among 2 different tipping landscapes and proposal for a potential third one.** The first landscape in light red, corresponds to the Hot-Warm House time interval. The second landscape in light blue, corresponds to the Cold-Ice house time interval. The third landscape, in light green, corresponds to the potential new one represented by the Anthropocene time interval. The different abrupt transitions identified in the present study are reported as TP or CT to differentiate the major tipping points from the critical transitions characterizing transitions of lighter significance in the climate history. Various plate tectonic and ice sheet events are indicated and supported by maps of plate movements and North and South Hemisphere ice sheets. The Antarctica maps are from Pollard and DeConto (2020), Northern Hemisphere ice sheet maps are from Batchelor et al. (2019). The paleogeographic maps have been generated using the Ocean Drilling Stratigraphic Network (ODSN) platetectonic reconstruction service: < https://www.odsn.de/odsn/services/paleomap/paleomap.html>. The red arrows on the tectonic maps indicate the key events at the identified abrupt transition.

References

Bagniewski, W., Ghil, M., and Rousseau, D. D.: Automatic detection of abrupt transitions in paleoclimate records, Chaos, 31, https://doi.org/10.1063/5.0062543, 2021.

Barker, S., Knorr, G., Edwards, R. L., Parrenin, F., Putnam, A. E., Skinner, L. C., Wolff, E., and Ziegler, M.: 800,000 Years of Abrupt Climate Variability, Science, 334, 347–351, https://doi.org/10.1126/science.1203580, 2011.

Batchelor, C. L., Margold, M., Krapp, M., Murton, D., Dalton, A. S., Gibbard, P. L., Stokes, C. R., Murton, J. B., and Manica, A.: The configuration of Northern Hemisphere ice sheets through the Quaternary, Nat. Commun., 10, https://doi.org/10.1038/s41467-019-11601-2, 2019.

Beerling, D. and Royer, D.: Convergent Cenozoic CO2 history, Nat. Geosci., 4, 418–420, https://doi.org/10.1038/ngeo1186, 2011.

Bialik, O., Frank, M., Betzler, C., Zammit, R., and Waldmann, N.: Two-step closure of the Miocene Indian Ocean Gateway to the Mediterranean, Sci. Rep., 9, https://doi.org/10.1038/s41598-019-45308-7, 2019.

Birkenmajer, K., Gaździcki, A., Krajewski, K. P., Przybycin, A., Solecki, A., Tatur, A., and Yoon, H. I.: First Cenozoic glaciers in west Antarctica, Pol. Polar Res., 3-12-3–12, 2005.

Birner, B., Hodell, D. A., Tzedakis, P. C., and Skinner, L. C.: Similar millennial climate variability on the Iberian margin during two early Pleistocene glacials and MIS 3, Paleoceanography, 31, 203–217, https://doi.org/10.1002/2015pa002868, 2016.

Boettner, C., Klinghammer, G., Boers, N., Westerhold, T., and Marwan, N.: Early-warning signals for Cenozoic climate transitions, Quat. Sci. Rev., 270, https://doi.org/10.1016/j.quascirev.2021.107177, 2021.

Bond, G., Heinrich, H., Broecker, W., Labeyrie, L., McManus, J., Andrews, J., Huon, S., Jantschik, R., Clasen, S., Simet, C., Tedesco, K., Klas, M., Bonani, G., and Ivy, S.: Evidence for massive discharges of icebergs into the North Atlantic Ocean during the last glacial period., Nature, 360, 245–249, 1992.

Broecker, W.: Climatic Change - Are we on the brink of a pronounced global warming, Science, 189, 460–463, https://doi.org/10.1126/science.189.4201.460, 1975.

Broecker, W. S. and Denton, G.: The role of ocean-atmosphere reorganizations in glacial cycles., Geochim Cosmochim Acta, 53, 2465–2501, 1989.

Broecker, W. S., Andree, M., Bonani, G., Wolfi, W., Oeschger, H., and Klas, M.: Can the Greenland climatic jumps be identified in records from ocean and land?, Quat. Res., 30, 1–6, 1988.

Brovkin, V., Brook, E., Williams, J., Bathiany, S., Lenton, T., Barton, M., DeConto, R., Donges, J., Ganopolski, A., McManus, J., Praetorius, S., de Vernal, A., Abe-Ouchi, A., Cheng, H., Claussen, M., Crucifix, M., Gallopin, G., Iglesias, V., Kaufman, D., Kleinen, T., Lambert, F., van der Leeuw, S., Liddy, H., Loutre, M., McGee, D., Rehfeld, K., Rhodes, R., Seddon, A., Trauth, M., Vanderveken, L., and Yu, Z.: Past abrupt

changes, tipping points and cascading impacts in the Earth system, Nat. Geosci., 14, 550–558, https://doi.org/10.1038/s41561-021-00790-5, 2021.

Chappell, J. and Shackleton, N. J.: Oxygen isotopes and sea-level, Nature, 324, 137–140, https://doi.org/10.1038/324137a0, 1986.

Cheng, H., Edwards, R. L., Sinha, A., Spotl, C., Yi, L., Chen, S. T., Kelly, M., Kathayat, G., Wang, X. F., Li, X. L., Kong, X. G., Wang, Y. J., Ning, Y. F., and Zhang, H. W.: The Asian monsoon over the past 640,000 years and ice age terminations, Nature, 534, 640–646, https://doi.org/10.1038/nature18591, 2016.

Clark, P. U. and Pollard, D.: Origin of the middle Pleistocene transition by ice sheet erosion of regolith, Paleoceanography, 13, 1–9, 1998.

Clark, P. U., Archer, D., Pollard, D., Blum, J. D., Rial, J. A., Brovkin, V., Mix, A. C., Pisias, N. G., and Roy, M.: The middle Pleistocene transition: characteristics. mechanisms, and implications for long-term changes in atmospheric PCO2, Quat. Sci. Rev., 25, 3150–3184, https://doi.org/10.1016/j.quascirev.2006.07.008, 2006.

Dansgaard, W., Johnsen, S. J., Moller, J., and Langway, C. C.: One thousand centuries of climatic record from Camp Century on the Greenland ice sheet., Science, 166, 377–381, 1969.

Dansgaard, W., Clausen, H. B., Gundestrup, N., Hammer, C. U. J., ohnsen, S. F., Kristinsdottir, P. M., and Reeh, N.: A new Greenland deep ice core., Science, 218, 1273–1277, 1982.

DeConto, R., Pollard, D., Wilson, P., Palike, H., Lear, C., and Pagani, M.: Thresholds for Cenozoic bipolar glaciation, Nature, 455, 652-U52, https://doi.org/10.1038/nature07337, 2008.

Dickens, G. R., Castillo, M. M., and Walker, J. C.: A blast of gas in the latest Paleocene: simulating first-order effects of massive dissociation of oceanic methane hydrate., Geology, 25 3, 259–62, 1997.

Eckmann, J. P., Kamphorst, S. O., and Ruelle, D.: Recurrence plots of dynamical systems, Europhys. Lett., 4, 973–977, https://doi.org/10.1209/0295-5075/4/9/004, 1987.

Efron, B.: nonparametric estimates of standard error - The Jackknife, the bootstrap and other methods, Biometrika, 68, 589–599, https://doi.org/10.2307/2335441, 1981.

Efron, B. and Tibshirani, R.: Bootstrap methods for standard errors, confidence intervals, and other measures of statistical accuracy, Stat. Sci., 1, 54–75, https://doi.org/10.1214/ss/1177013815, 1986.

Elderfield, H., Ferretti, P., Greaves, M., Crowhurst, S., McCave, I. N., Hodell, D., and Piotrowski, A. M.: Evolution of Ocean Temperature and Ice Volume Through the Mid-Pleistocene Climate Transition, Science, 337, 704–709, https://doi.org/10.1126/science.1221294, 2012.

Gulick, S., Barton, P., Christeson, G., Morgan, J., McDonald, M., Mendoza-Cervantes, K., Pearson, Z., Surendra, A., Urrutia-Fucugauchi, J., Vermeesch, P., and Warner, M.: Importance of pre-impact crustal structure for the asymmetry of the Chicxulub impact crater, Nat. Geosci., 1, 131–135, https://doi.org/10.1038/ngeo103, 2008.

Gulick, S., Christeson, G., Barton, P., Grieve, R., Morgan, J., and Urrutia-Fucugauchi, J.: Geophysical characterization of the Chicxulub impact crater, Rev. Geophys., 51, 31–52, https://doi.org/10.1002/rog.20007, 2013.

Gulick, S., Shevenell, A., Montelli, A., Fernandez, R., Smith, C., Warny, S., Bohaty, S., Sjunneskog, C., Leventer, A., Frederick, B., and Blankenship, D.: Initiation and long-term instability of the East Antarctic Ice Sheet, Nature, 552, 225-+, https://doi.org/10.1038/nature25026, 2017.

Gulick, S., Bralowe, T., Ormo, J., Hall, B., Grice, K., Schaefer, B., Lyons, S., Freeman, K., Morgan, J., Artemieva, N., Kaskes, P., de Graaff, S., Whalen, M., Collins, G., Tikoo, S., Verhagen, C., Christeson, G., Claeys, P., Coolen, M., Goderis, S., Goto, K., Grieve, R., McCall, N., Osinski, G., Rae, A., Biller, U., Smit, J., Vajda, V., Wittmann, A., and Expedition 364 Scientists: The first day of the Cenozoic, Proc. Natl. Acad. Sci. U. S. A., 116, 19342–19351, https://doi.org/10.1073/pnas.1909479116, 2019.

Hodell, D. A. and Channell, J. E. T.: Mode transitions in Northern Hemisphere glaciation: co-evolution of millennial and orbital variability in Quaternary climate, Clim. Past, 12, 1805–1828, https://doi.org/10.5194/cp-12-1805-2016, 2016.

Hoffman, P. F., Abbot, D. S., Ashkenazy, Y., Benn, D. I., Brocks, J. J., Cohen, P. A., Cox, G. M., Creveling, J. R., Donnadieu, Y., Erwin, D. H., Fairchild, I. J., Ferreira, D., Goodman, J. C., Halverson, G. P., Jansen, M. F., Le Hir, G., Love, G. D., Macdonald, F. A., Maloof, A. C., Partin, C. A., Ramstein, G., Rose, B. E. J., Rose, C. V., Sadler, P. M., Tziperman, E., Voigt, A., and Warren, S. G.: Snowball Earth climate dynamics and Cryogenian geology-geobiology, Sci. Adv., 3, https://doi.org/10.1126/sciadv.1600983, 2017.

IPCC: Climate Change 2021: The Physical Science Basis. Contribution of Working Group I to the Sixth Assessment Report of the Intergovernmental Panel on Climate Change, Cambridge University Press, Cambridge, United Kingdom and New York, NY, USA, https://doi.org/10.1017/9781009157896, 2021.

Janis, C.: Tertiary mammal evolution in the context of changing climates, vegetation, and tectonic events, Annu. Rev. Ecol. Syst., 24, 467–500, https://doi.org/10.1146/annurev.es.24.110193.002343, 1993.

Jolley, D. W. and Bell, B. R.: The North Atlantic Igneous Province: Stratigraphy, Tectonic, Volcanic, and Magmatic Processes, 2002.

Kennett, J. and Shackleton, N.: Oxugen isotopic evidence for development of psychrosphere 38 Myr ago, Nature, 260, 513–515, https://doi.org/10.1038/260513a0, 1976.

Kennett, J. and Stott, L.: Abrupt deep-sea warming, palaeoceanographic changes and benthic extinctions at the end of the Paleocene, Nature, 353, 225–229, https://doi.org/10.1038/353225a0, 1991.

Kriegler, E., Hall, J., Held, H., Dawson, R., and Schellnhuber, H.: Imprecise probability assessment of tipping points in the climate system, Proc. Natl. Acad. Sci. U. S. A., 106, 5041–5046, https://doi.org/10.1073/pnas.0809117106, 2009.

Lagabrielle, Y., Godderis, Y., Donnadieu, Y., Malavieille, J., and Suarez, M.: The tectonic history of Drake Passage and its possible impacts on global climate, Earth Planet. Sci. Lett., 279, 197–211, https://doi.org/10.1016/j.epsl.2008.12.037, 2009.

Lenton, T.: Environmental Tipping Points, in: Annual review of Environment and Resources, vol. 38, edited by: Gadgil, A. and Liverman, D., 1–29, https://doi.org/10.1146/annurev-environ-102511-084654, 2013.

Lenton, T. and Williams, H.: On the origin of planetary-scale tipping points, TRENDS Ecol. Evol., 28, 380–382, https://doi.org/10.1016/j.tree.2013.06.001, 2013.

Lenton, T., Held, H., Kriegler, E., Hall, J., Lucht, W., Rahmstorf, S., and Schellnhuber, H.: Tipping elements in the Earth's climate system, Proc. Natl. Acad. Sci. U. S. A., 105, 1786–1793, https://doi.org/10.1073/pnas.0705414105, 2008.

Lenton, T., Rockstrom, J., Gaffney, O., Rahmstorf, S., Richardson, K., Steffen, W., and Schellnhuber, H.: Climate tipping points - too risky to bet against, Nature, 575, 592–595, https://doi.org/10.1038/d41586-019-03595-0, 2019.

Lenton, T., Benson, S., Smith, T., Ewer, T., Lanel, V., Petykowski, E., Powell, T., Abrams, J., Blomsma, F., and Sharpe, S.: Operationalising positive tipping points towards global sustainability, Glob. Sustain., 5, https://doi.org/10.1017/sus.2021.30, 2022.

Lomax, B., Beerling, D., Upchurch, G., and Otto-Bliesner, B.: Rapid (10-yr) recovery of terrestrial productivity in a simulation study of the terminal Cretaceous impact event, Earth Planet. Sci. Lett., 192, 137–144, https://doi.org/10.1016/S0012-821X(01)00447-2, 2001.

Lunt, D., Valdes, P., Haywood, A., and Rutt, I.: Closure of the Panama Seaway during the Pliocene: implications for climate and Northern Hemisphere glaciation, Clim. Dyn., 30, 1–18, https://doi.org/10.1007/s00382-007-0265-6, 2008.

Marwan, N., Carmen Romano, M., Thiel, M., and Kurths, J.: Recurrence plots for the analysis of complex systems, Phys. Rep., 438, 237–329, https://doi.org/10.1016/j.physrep.2006.11.001, 2007.

Marwan, N., Schinkel, S., and Kurths, J.: Recurrence plots 25 years later - Gaining confidence in dynamical transitions, EPL, 101, https://doi.org/10.1209/0295-5075/101/20007, 2013.

Milankovic, M.: Théorie mathématique des Phénomènes thermiques produits par la radiation solaire, edited by: Académie Yougoslave des Sciences et des Arts de Zagreb, Gauthier Villars, Paris, 1920.

Milankovic, M.: Kanon der Erdbestrahlung und seine Anwendung auf das Eiszeitenproblem, Royal Serbian Sciences, Belgrade, 633p pp., 1941.

Miller, K., Browning, J., Schmelz, W., Kopp, R., Mountain, G., and Wright, J.: Cenozoic sea-level and cryospheric evolution from deep-sea geochemical and continental margin records, Sci. Adv., 6, https://doi.org/10.1126/sciadv.aaz1346, 2020.

O'Keefe, J. D. and Ahrens, T. J.: Impact production of C02 by the Cretaceous/Tertiary extinction bolide and the resultant heating of the Earth, Nature, 338, 247–249, https://doi.org/10.1038/338247a0, 1989.

Otto, I., Donges, J., Cremades, R., Bhowmik, A., Hewitte, R., Lucht, W., Rockstrom, J., Allerberger, F., McCaffrey, M., Doe, S., Lenferna, A., Moran, N., van Vuuren, D., and Schellnhuber, H.: Social tipping dynamics for stabilizing Earth's climate by 2050, Proc. Natl. Acad. Sci. U. S. A., 117, 2354–2365, https://doi.org/10.1073/pnas.1900577117, 2020.

Palike, H., Lyle, M., Nishi, H., Raffi, I., Ridgwell, A., Gamage, K., Klaus, A., Acton, G., Anderson, L., Backman, J., Baldauf, J., Beltran, C., Bohaty, S., Bown, P., Busch, W., Channell, J., Chun, C., Delaney, M., Dewangan, P., Dunkley Jones, T., Edgar, K., Evans, H., Fitch, P., Foster, G., Gussone, N., Hasegawa, H., Hathorne, E., Hayashi, H., Herrle, J., Holbourn, A., Hovan, S., Hyeong, K., Iijima, K., Ito, T., Kamikuri, S., Kimoto, K., Kuroda, J., Leon-Rodriguez, L., Malinverno, A., Moore, T., Murphy, B., Murphy, D., Nakamura, H., Ogane, K., Ohneiser, C., Richter, C., Robinson, R., Rohling, E., Romero, O., Sawada, K., Scher, H., Schneider, L., Sluijs, A., Takata, H., Tian, J., Tsujimoto, A., Wade, B., Westerhold, T., Wilkens, R., Williams, T., Wilson, P., Yamamoto, Y., Yamamoto, S., Yamazaki, T., and Zeebe, R.: A Cenozoic record of the equatorial Pacific carbonate compensation depth, Nature, 488, 609-+, https://doi.org/10.1038/nature11360, 2012.

Pisias, N. G. and Moore, T. C.: The evolution of Pleistocene climate: A time-series approach, Earth Planet. Sci. Lett., 52, 450–458, https://doi.org/10.1016/0012-821x(81)90197-7, 1981.

Pollard, D. and DeConto, R.: Continuous simulations over the last 40 million years with a coupled Antarctic ice sheet-sediment model, Palaeoclimatol. Palaeoecol. Palaeogeogr., 537, https://doi.org/10.1016/j.palaeo.2019.109374, 2020.

Rasmussen, S. O., Bigler, M., Blockley, S. P., Blunier, T., Buchardt, S. L., Clausen, H. B., Cvijanovic, I., Dahl-Jensen, D., Johnsen, S. J., Fischer, H., Gkinis, V., Guillevic, M., Hoek, W. Z., Lowe, J. J., Pedro, J. B., Popp, T., Seierstad, I. K., Steffensen, J. P., Svensson, A. M., Vallelonga, P., Vinther, B. M., Walker, M. J. C., Wheatley, J. J., and Winstrup, M.: A stratigraphic framework for abrupt climatic changes during the Last Glacial period based on three synchronized Greenland ice-core records: refining and extending the INTIMATE event stratigraphy, Quat. Sci. Rev., 106, 14–28, https://doi.org/10.1016/j.quascirev.2014.09.007, 2014.

Rose, K., Ferraccioli, F., Jamieson, S., Bell, R., Corr, H., Creyts, T., Braaten, D., Jordan, T., Fretwell, P., and Damaske, D.: Early East Antarctic Ice Sheet growth recorded in the landscape of the Gamburtsev Subglacial Mountains, Earth Planet. Sci. Lett., 375, 1–12, https://doi.org/10.1016/j.epsl.2013.03.053, 2013.

Rousseau, D., Bagniewski, W., and Ghil, M.: Abrupt climate changes and the astronomical theory: are they related?, Clim. Past, 18, 249–271, https://doi.org/10.5194/cp-18-249-2022, 2022.

Rousseau, D.-D., Antoine, P., Boers, N., Lagroix, F., Ghil, M., Lomax, J., Fuchs, M., Debret, M., Hatté, C., Moine, O., Gauthier, C., Jordanova, D., and Jordanova, N.: Dansgaard-Oeschger-like events of the penultimate climate cycle: The loess point of view, Clim. Past, 16, 713–727, https://doi.org/10.5194/cp-16-713-2020, 2020.

Rowley, D. and Currie, B.: Palaeo-altimetry of the late Eocene to Miocene Lunpola basin, central Tibet, Nature, 439, 677–681, https://doi.org/10.1038/nature04506, 2006.

Ruddiman, W. F., Raymo, M., Martinson, D. G., Clement, B. M., and Backman, J.: Pleistocene evolution : Northern Hemisphere ice sheets and North Atlantic Ocean., Paleoceanography, 4, 353–412, 1989.

Scotese, C. R., Song, H., Mills, B. J. W., and van der Meer, D. G.: Phanerozoic paleotemperatures: The earth's changing climate during the last 540 million years, Earth-Sci. Rev., 215, https://doi.org/10.1016/j.earscirev.2021.103503, 2021.

Shackleton, N. J.: Oceanic Carbon Isotope Constraints on Oxygen and Carbon Dioxide in the Cenozoic Atmosphere, in: The Carbon Cycle and Atmospheric CO2: Natural Variations Archean to Present, American Geophysical Union (AGU), 412–417, https://doi.org/10.1029/GM032p0412, 1985.

Shackleton, N. J.: The 100,000-year ice-age cycle identified and found to lag temperature, carbon dioxide, and orbital eccentricity, Science, 289, 1897–1902, https://doi.org/10.1126/science.289.5486.1897, 2000.

Shackleton, N. J. and Opdyke, N. D.: Oxygen isotope and palaeomagnetic evidence for early Northern Hemisphere glaciation., Nature, 270, 216–223, 1977.

Steffen, W., Rockstrom, J., Richardson, K., Lenton, T., Folke, C., Liverman, D., Summerhayes, C., Barnosky, A., Cornell, S., Crucifix, M., Donges, J., Fetzer, I., Lade, S., Scheffer, M., Winkelmann, R., and Schellnhuber, H.: Trajectories of the Earth System in the Anthropocene, Proc. Natl. Acad. Sci. U. S. A., 115, 8252–8259, https://doi.org/10.1073/pnas.1810141115, 2018.

Thomas, E., Zachos, J. C., and Bralower, T. J.: Deep-sea environments on a warm earth: latest Paleocene-early Eocene, in: Warm Climates in Earth History, edited by: Huber, B. T., Macleod, K. G., and Wing, S. L., Cambridge University Press, Cambridge, 132–160, https://doi.org/10.1017/CBO9780511564512.006, 1999.

Torsvik, T. H. and Cocks, L. R. M.: Earth history and palaeogeography, Cambridge University Press, 2016.

Turner, S. K.: Pliocene switch in orbital-scale carbon cycle/climate dynamics, Paleoceanography, 29, 1256–1266, https://doi.org/10.1002/2014pa002651, 2014.

Wang, Y. J., Cheng, H., Edwards, R. L., An, Z. S., Wu, J. Y., Shen, C. C., and Dorale, J. A.: A high-resolution absolute-dated Late Pleistocene monsoon record from Hulu Cave, China, Science, 294, 2345–2348, https://doi.org/10.1126/science.1064618, 2001.

Westerhold, T., Marwan, N., Drury, A. J., Liebrand, D., Agnini, C., Anagnostou, E., Barnet, J. S. K., Bohaty, S. M., De Vleeschouwer, D., Florindo, F., Frederichs, T., Hodell, D. A., Holbourn, A. E., Kroon, D., Lauretano, V., Littler, K., Lourens, L. J., Lyle, M., Palike, H., Rohl, U., Tian, J., Wilkens, R. H., Wilson, P. A., and Zachos, J. C.: An astronomically dated record of Earth's climate and its predictability over the last 66 million years, Science, 369, 1383-+, https://doi.org/10.1126/science.aba6853, 2020.

Wunderling, N., Donges, J., Kurths, J., and Winkelmann, R.: Interacting tipping elements increase risk of climate domino effects under global warming, Earth Syst. Dyn., 12, 601–619, https://doi.org/10.5194/esd-12-601-2021, 2021.

Zachos, J., Breza, J., and Wise, S.: Early Oligocene ice-sheet expansion on Antractica - stable isotope and sedimentological evidence from Kerguelen Plateau, Southern Indian-Ocean, Geology, 20, 569–573, https://doi.org/10.1130/0091-7613(1992)020<0569:EOISEO>2.3.CO;2, 1992.

Zachos, J., Pagani, M., Sloan, L., Thomas, E., and Billups, K.: Trends, rhythms, and aberrations in global climate 65 Ma to present, Science, 292, 686–693, 2001.

Fig. 1

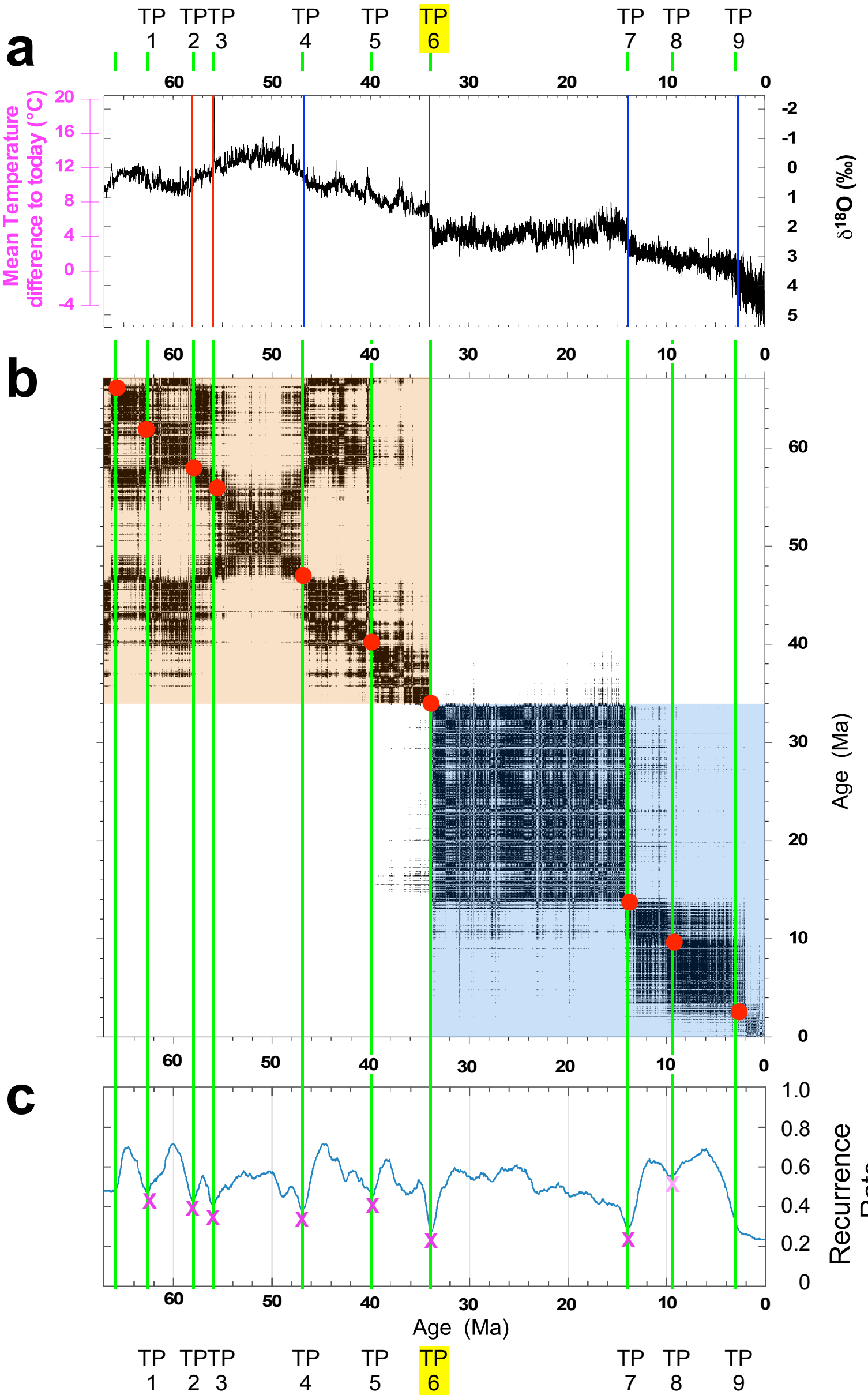
a
TP 1
TP 2
TP 3
TP 4
TP 5
TP 6
TP 7
TP 8
TP 9
60
50
40
30
20
10
0
Mean Temperature difference to today (°C)
20
16
12
8
4
0
-4
-2
-1
0
1
2
3
4
5
δ18O (‰)
b
60
50
40
30
20
10
0
Age (Ma)
c
1.0
0.8
0.6
0.4
0.2
0
Recurrence Rate
Age (Ma)

Fig. 2

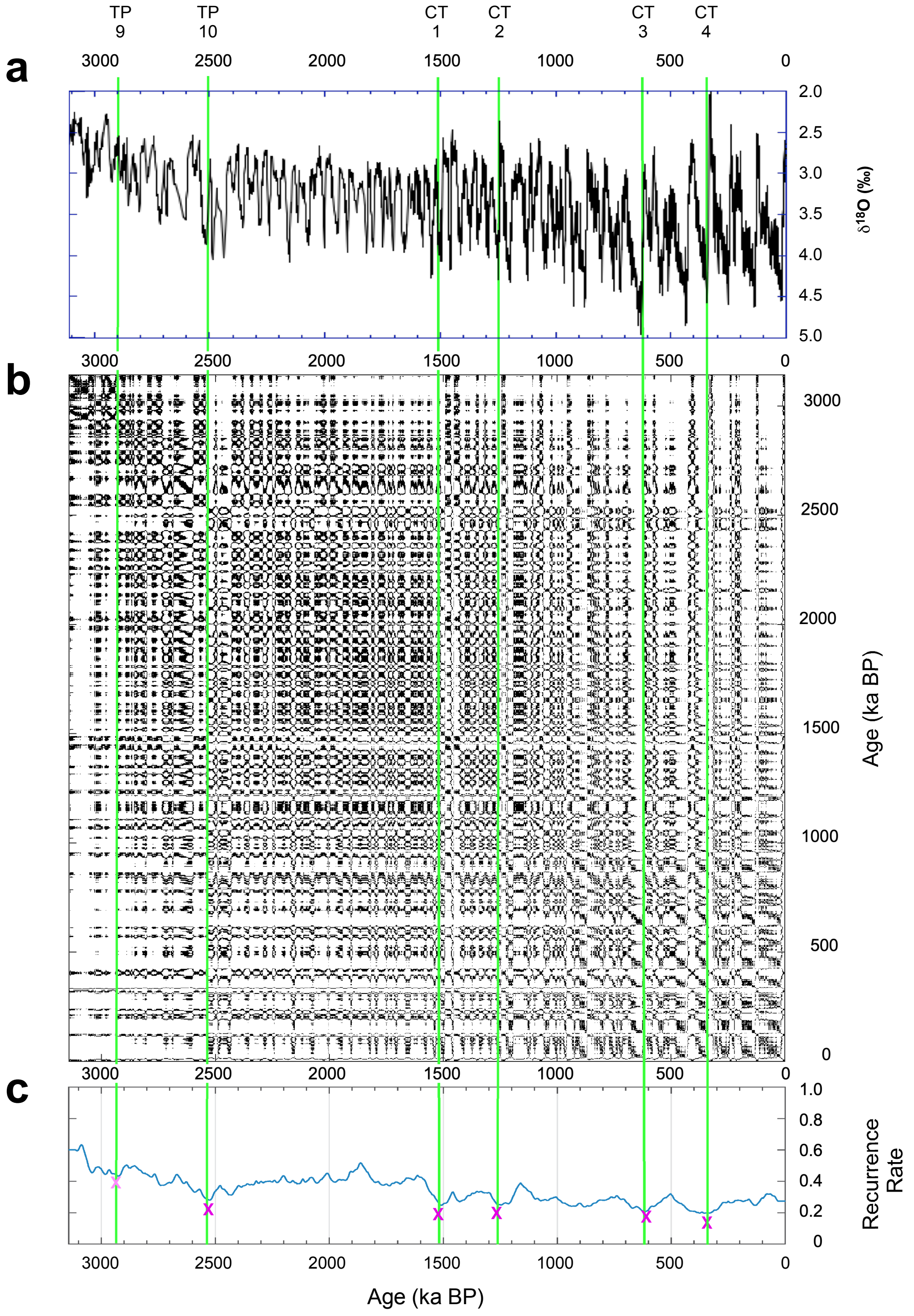
a
TP 9
TP 10
CT 1
CT 2
CT 3
CT 4
3000
2500
2000
1500
1000
500
0
2.0
2.5
3.0
3.5
4.0
4.5
5.0
δ18O (‰)
b
3000
2500
2000
1500
1000
500
0
Age (ka BP)
c
1.0
0.8
0.6
0.4
0.2
0
Recurrence Rate
Age (ka BP)

Fig. 3

a

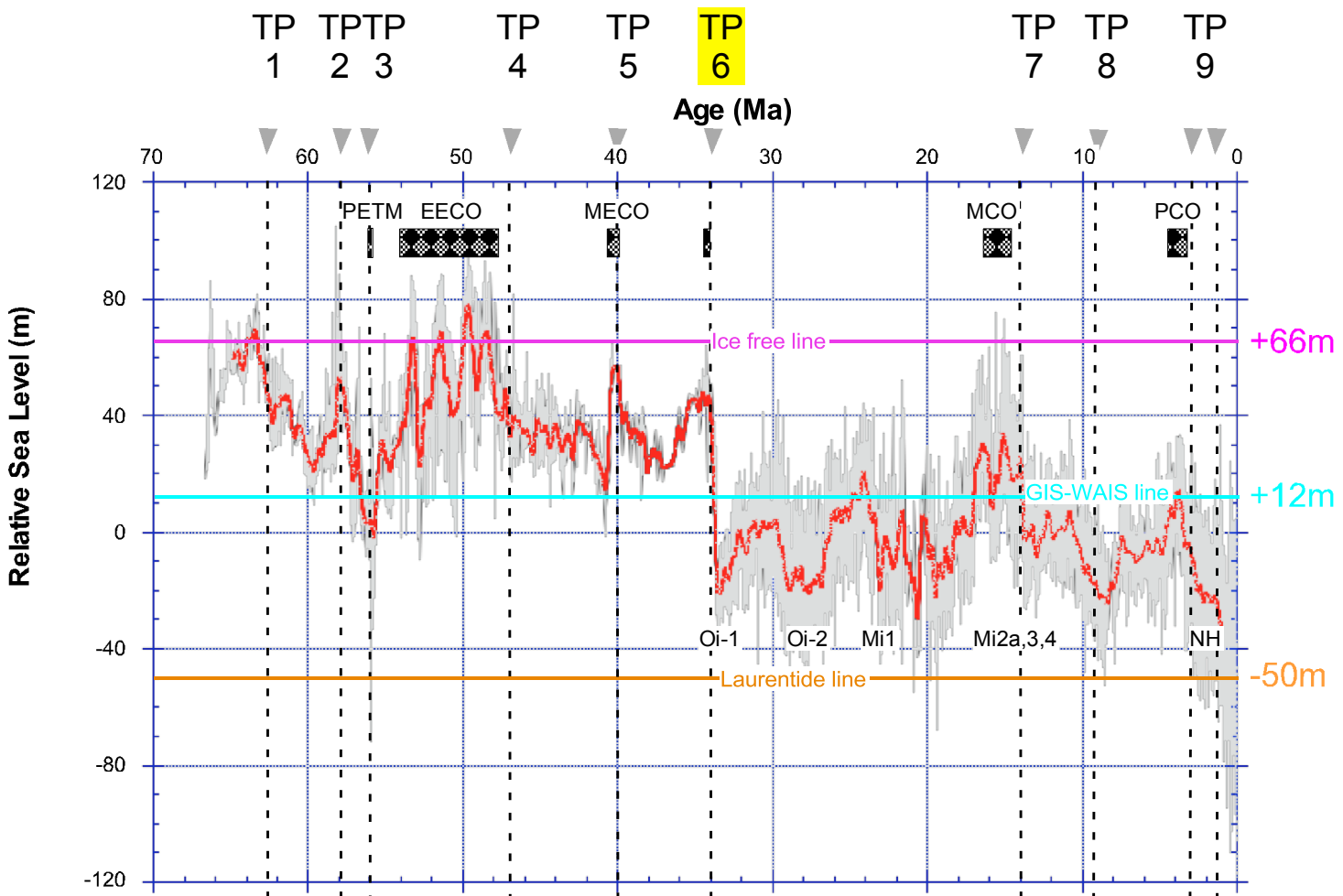
TP 1
TP 2
TP 3
TP 4
TP 5
TP 6
TP 7
TP 8
TP 9
Age (Ma)
70
60
50
40
30
20
10
0
Relative Sea Level (m)
120
80
40
0
-40
-80
-120
PETM
EECO
MECO
MCO
PCO
Ice free line
+66m
GIS-WAIS line
+12m
Oi-1
Oi-2
Mi1
Mi2a,3,4
NH
Laurentide line
-50m

b


Paleodepth (m)
2500
3000
3500
4000
4500
5000
eq CCD(m)
off-eq CCD (m)

c

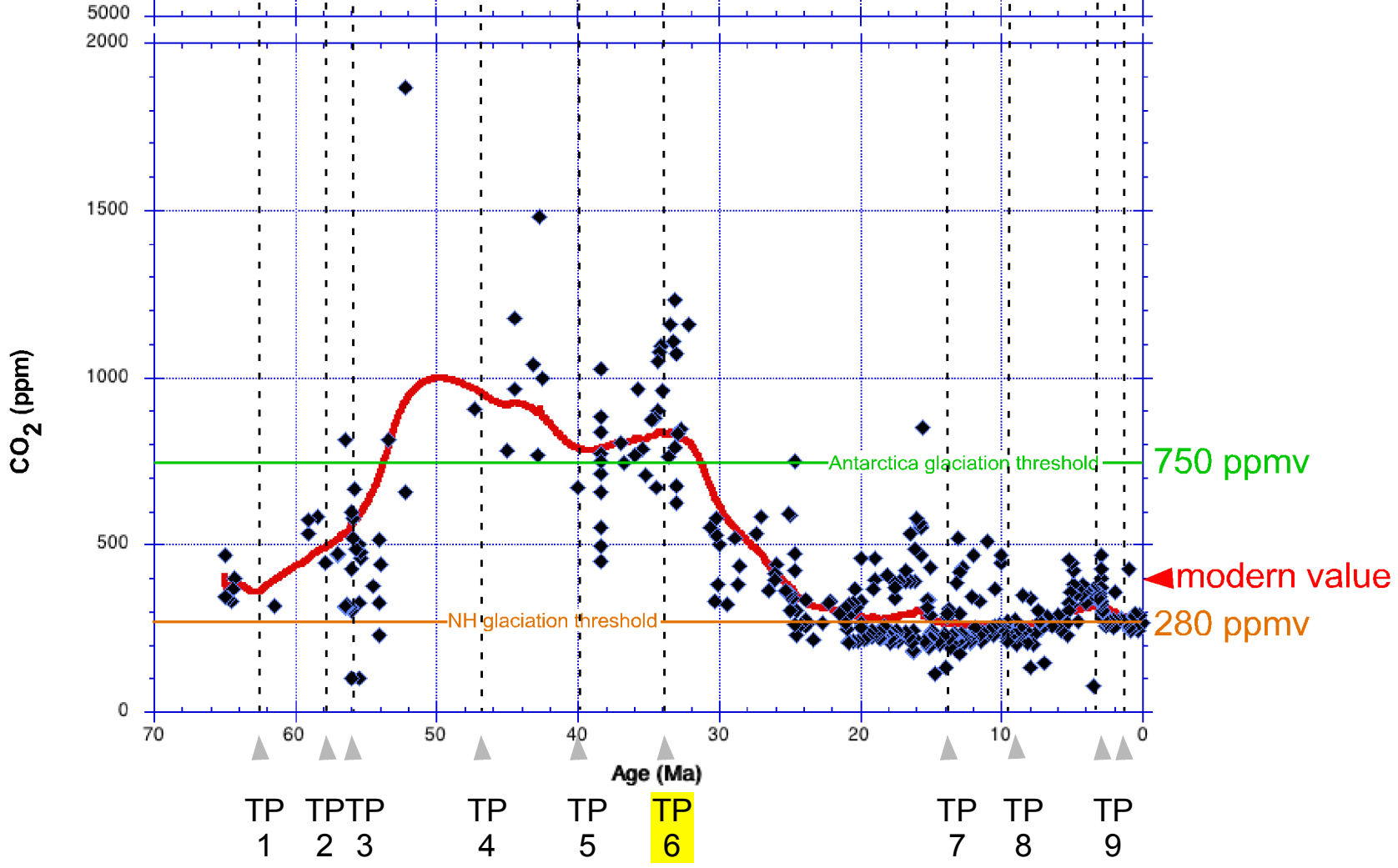
CO_2 (ppm)
2000
1500
1000
500
0
Antarctica glaciation threshold
750 ppmv
modern value
NH glaciation threshold
280 ppmv
70
60
50
40
30
20
10
0
Age (Ma)
TP 1
TP 2
TP 3
TP 4
TP 5
TP 6
TP 7
TP 8
TP 9

Fig. 5

Hot - Warm house landscape

Chicxulub Meteorit impact
Deccan traps

LDC

TP 62 Ma

Increasing C02

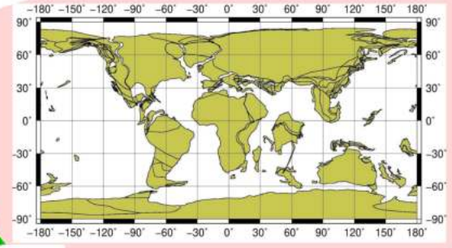

Onset of hothouse

TP 58-56 Ma PETM

Shallow depth of CDD (about 3km)
+ CO2 increasing
North Atlantic Igneous Province

Max C02

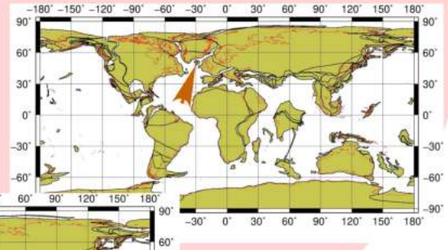

Onset of Warmhouse world
Deepening of CDD

TP 47 Ma

Several meteorite impacts:
-Chesapeake Bay (35.5Ma)
-Popigai (35.7Ma)
- N continental migrations

icing of Antarctica

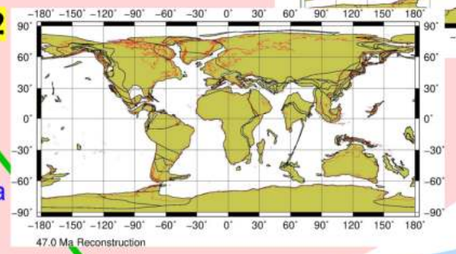

Onset of Cold world

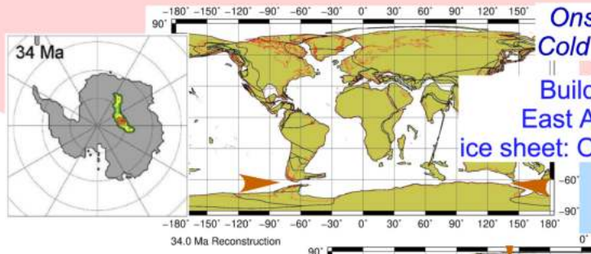

TP6 34 Ma EOT

Drake and Tasmanian passages opening
Fall in relative sea-level & strong deepening of CDD (>1km)
+ deep sea tp drop (change in MOC), decrease in SH deep water formation strength
CO2 threshold

Decreasing C02

Build up of East Antarctic ice sheet: Oi-1 glaciation

TP 14 Ma MMCT

Closure of Tethyan seaway & Indonesian gateway
End of Columbia River volcanism Andes uplift & deepening of CDD

Build up of W Antarctic ice sheet and reinforcement of EAIS

TP 2.9-2.5 Ma

Closure of Panama Isthmus
Eustatic fall of 14m at the end of MPWP & deepening of CDD

Build up of NH glaciers/ice sheets

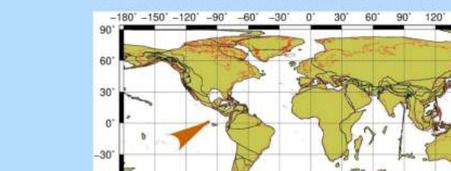

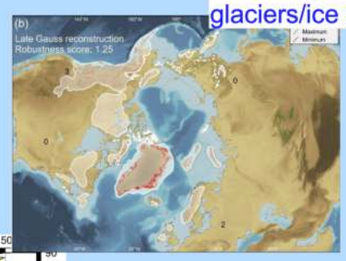

CT 1.5 Ma Regular IRDs during glacials

Massive size & expansion of N Hemisphere continental ice sheets

CT 1.22-0.9 Ma Mid-Pleistocene transition: 40 kyr to 100 kyr

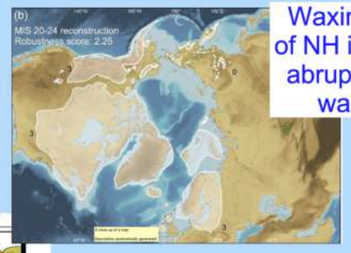

Waxing-vaning of NH ice-sheets: abrupt DO-like warmings

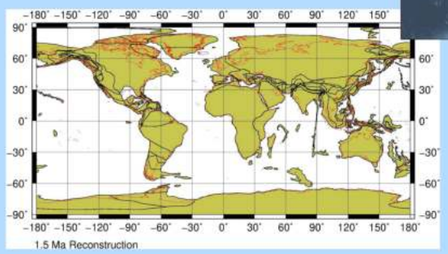

Maximum size of N Hemisphere continental ice sheets

CT 0.65 Ma Heinrich events during glacials Bond cycles

Holocene-IE
Bond events

Cool - Ice house landscape

New Anthropocene landscape?

IPCC scenarios of global warming

Greenland and W Antarctica collapses
TP7
2050-2100?
MV-> IPCC scenarios

Increasing C02

NH Hemisphere ice sheet collapses

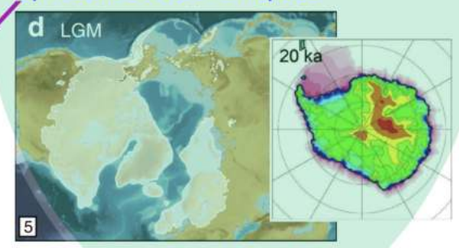

Supplementary Text

Comparison between GMSL, CCD and CO2 concentration from CENOGRID (past 66 Myr)

The interval between 66 Ma and 63 Ma (TP1) shows a relative stable GMSL above +60m. It is followed by a lowering corresponding to a decreasing trend of about 70m in several steps between TP1 at 63 Ma and TP3 at 56 Ma, punctuated by an abrupt increase of 52m, at TP2 around 58 Ma, and another of 28m corresponding to the short but intense Paleocene-Eocene Thermal Maximum (PETM – Fig. 3a) warming. GMSL raises between TP2 at 58 Ma and 55 Ma by about +40m. The interval between 55 Ma and 48 Ma, the Early Eocene climatic optimum (EEOC – Fig. 3a), indicates a relatively high GMSL of about 66 m above the present mean sea level, which is associated with the occurrence of hyperthermal conditions at 58 Ma, 57 Ma, 53 Ma. Between 52 Ma and TP4 at about 47 Ma, CCD reaches the shallowest depth of the record, about 3000m, (Palike et al., 2012)) associated with the highest CO_2 concentrations estimated above 1100 ppmv by Beerling & Royer (2011)– Fig. 3b,c). A strong decrease in GMSL of about 30m occurs between 48 Ma and 46 Ma while it remains relatively stable at about +42m between 46 Ma and TP5, at 40 Ma. It is however punctuated by two short events, first a lowering of about 25m between 42 Ma and 40.5 Ma, and strong increase of about 40m between 40.5 Ma and 40 Ma (TP5) corresponding to the Middle Eocene Climatic optimum (MECO – Fig. 3a). A two-step lowering of about 35m of the GMSL occurs between 40 Ma (TP5) and 36 Ma, followed by a gradual increase of about 25m between 36 Ma and 34.5 Ma just before the Eocene-Oligocene Transition (EOT – Fig. 3a). Between 46 Ma and 34 Ma (TP6), the CCD is strongly oscillating with numerous deepening events of 500 to 1000 m magnitude and shoaling ones, corresponding to carbonate accumulation episodes. These oscillations in the CCD occurred during an interval indicating still high CO_2 concentrations, roughly above the 750 ppmv considered as an Antarctic glaciation threshold (DeConto et al., 2008), and marked by a relative minimum at about TP5 at 40 Ma (Fig. 3b,c). This first interval of the GMSL, ending by the strong deepening of about 1000m associated with a strong decrease in CO_2 concentration, determines variations of a rather completely ice free Earth, at least with no major ice sheet either in southern and northern hemisphere. This is deduced first from the high GMSL, mainly above 12m (Fig. 4a), which would correspond to the mutual contribution of the Greenland and the West Antarctic ice sheets, and second from high CO_2 concentrations estimates in agreement with a CCD generally lower than 4000 m (Fig 3b, c).

The second main interval shows a completely different scenario with the GMSL varying between +30m and -80m without considering the late Quaternary interval, and much lower CCD and CO_2 concentration (Fig. 3b,c. First the strong decrease in the GMSL at EOT reaches negative values of about -25m at about 33.5Ma. It is interpreted as the evidence of the first continental scale Antarctic ice sheet (first Oligocene isotope maximum - Oi1 – Fig. 3a) (Miller et al., 1991). After a return to values similar to present mean sea level, about +2m, between 32 Ma and 30 Ma, a new decreases of about 25m in GMSL is occurring between 29.5 Ma and 27 Ma corresponding to another continental scale Antarctic ice sheet extent labeled Oi2 (Fig.

3a). After a two-step increase in GMSL of about 40m between 27 Ma and 24 Ma, a new sharp decrease of about 40m is noticed at about 23 Ma. It corresponds to the Middle Oligocene Maximum (Mi1 – Fig. 3a), another Antarctic ice sheet wide expansion (Miller et al., 1991; Boulila et al., 2011). From TP6, at 34 Ma, and 23 Ma, the CO_2 concentration decreases associated with a deepening trend in the CCD down to about -4600m. From 23 Ma until about 19 Ma, GMSL shows oscillations but with lower values than present day at about -20m, whereas from 19 Ma until 17 Ma, GMSL increases by about 50m to indicate high values around +30 m above present day value (Fig. 3a). The CCD indicates about 600 m shoaling which lasted around 2.5 Myr linked to some high estimates of CO_2 concentration (from paleosols, stomata) (Beerling and Royer, 2011) (Fig. 3b,c). This strong increase corresponds to the Miocene Climatic optimum (MCO – Fig. 3a), between 17 Ma and TP7 at 13.9 Ma, which is the last interval during which GMSL reaches such high values (higher than +20m) above the present day ones (Fig. 3). The interval between TP7 at 13.9 Ma and 13 Ma corresponds to the Middle Miocene transition during which GMSL decreases once more significantly by about 35m. Such lowering is associated with the growth of the East Antarctic ice sheet to near its present state, remaining a perennial ice body that is thereafter impacting the Earth climate (Paxman et al., 2019; Pollard and DeConto, 2020). Although GMSL remains relatively stable between 13 Ma and 12 Ma, another strong decrease, again of about 30m, occurs between TP8 at about 9 Ma and 8.5 Ma, associated with the strongest deepening recorded by the CCD, around 4800m. GMSL increases again by about 20m until 7.5 Ma to remain relatively stable until 5.5 Ma when GMSL increases by about 20m between 5.5 Ma and 3.5 Ma, corresponding to the Pliocene Climatic Optimum (PCO – Fig. 3a). Between 3.5 Ma until TP9 at about 2.7 Ma GMSL shows a sharp decreasing trend of about 35m (Mi2a, 3, 4 – Fig. 3a) with the initiation of the development of the large northern ice sheets between 2.9 Ma (TP9) and 2.5 Ma (TP10 – Fig. 2), especially the Laurentide ice sheet corresponding to about 50m decrease of GMSL with regards to the present day value (Fig. 3a). From TP8 at about 9 onward, CCD shows fluctuations although remaining at around 4500m with two strong deepening at about TP9 2.9 Ma and TP10 (Fig. 3) at 2.5 Ma.

In another global sea level reconstruction, Rohling et al. (2021) individualized several major thresholds that agree with Miller et al (2020) reconstruction and our present analysis. Indeed they estimate the EOT global sea level drop at 34 Ma (TP6) as being of about between 30m, while previously reconstructed of 70m-80m by Houben et al. (2012), and by Miller et al. (2020). They also estimate this drop in global sea level being associated to a 2.5°C cooling interpreted previously as above the onset of the Antarctic ice sheet glaciation. Rohling et al. (2021) also identify 14 Ma (TP7) threshold as the end of the last intermittently ice free period of the Earth history of the last 40 Ma with only southern hemisphere ice sheets impacting the Earth climate. Miller et al. (2020) indicate a 35m lowering at that particular transition. Indeed Rohling et al (2021) indicate a slight sea level negative shift at about 10 Ma (TP8), of about 10m for Miller et al. (2020), as the onset of partial or ephemeral northern Hemisphere ice bodies

with 2 other sea level threshold at about 3 (about TP9) and 2.75 (TP10), also observed in Miller et al. (Miller et al., 2020). These two key dates correspond to respectively the first major iceberg calving in the Nordic Seas (Smith et al., 2018) and from the Laurentide ice sheet (Bailey et al., 2013) although this interpretation was rejected by Naaf et al. (2013) reviewing N Atlantic ice rafted records, and rather attributing the IRD signature to Greenland and Fennoscandian glaciers. Hodell and Channell (2016) identified the first occurrence of iceberg calving in North Atlantic at about 2.75 from the analysis of the $d^{18}O$ of benthic bulk carbonate in core U1308 (Supp. Fig. 3), a date identified as an abrupt transition in the RR analysis of both $\delta^{18}O$ of benthic foram and bulk carbonate (Rousseau et al., 2022). All along the past 66 Ma, GMSL has been varying between average values of 38.47 m ± 14.85 m above the present day value during the hotworld interval prior TP 6 at 34 Ma, and of -3.49m ± 12.90m after 34 Ma until present day during the coldworld interval (Tab. 2).

The past 3.3 Myr (from (Rousseau et al., 2022)**.**

The first date, TP10 detected by RQA, is interpreted as corresponding to the earliest occurrence of IRD in the North Atlantic. This occurrence characterizes the presence of Northern Hemisphere coastal glaciers large enough to calve icebergs in the ocean, and the melting of these icebergs is likely to have impacted the oceanic circulation. Naafs et al. (2013), however, reported the occurrence of weak IRD events in the late Pliocene that they attributed mainly to Greenland and Fennoscandian glaciers. Such interpretation points to nevertheless smaller ice sheets over these regions than during the later Quaternary, when North American ice sheets were considerably larger. The interval TP9, at 2.8 Ma, to CT2, at 1.2 Ma, shows glacial–interglacial sea level variations of about 25–50 m below the present day. The CO_2 concentrations varied between 270 ppmv and 280 ppmv during interglacials and between 210 ppmv and 240 ppmv during glacials, with a decreasing trend of about 23 ppmv over this 1.4-Myr–long interval (van de Wal et al., 2011).

The second date, CT1, at 1.55 Ma, corresponds to an increased amplitude in ice volume variations between glacial minima and interglacial optima. This second step shows the permanent occurrence of ice-rafted events during glacial intervals in the record (Suppl. Fig. 3), therefore an amplified relationship of climate variations with Northern Hemisphere ice sheets. The increase in IRD variability and magnitude since CT1, however, shows that distinct, faster processes have to be considered than those due to slow changes in Earth's orbital parameters; see again Fig. 2.

The third date, CT2, at 1.25 Ma, close to the MIS22–24 $\delta^{18}O$ optima, shows increased continental ice volume in the Northern Hemisphere (Batchelor et al., 2019), but also more stability in the East Antractic ice sheet in Southern Hemisphere (Jakob et al., 2020). In parallel, evidence of a major glacial pulse recorded in Italy's Po Plain, as well as in ^{10}Be-dated boulders in Switzerland, is interpreted as marking the onset of the first major glaciation in the Alps (Muttoni et al., 2003; Knudsen et al., 2020).

After CT2, at1.25 Ma, the sea level changes decreased to about 70–120 m below the present day, while the CO_2 concentrations varied between 250 ppmv and 320 ppmv during interglacials and between 170 ppmv and 210 ppmv during glacials (Berends et al., 2021). Similar variations were determined by Seki et al. (2010), although pCO_2 changes that occurred before the time reached by ice core records are associated with high uncertainties in both dating and values. The sawtooth pattern of the interglacial– glacial cycles (Broecker and van Donk, 1970) becomes noticeable at 0.9 Ma. At about the same time, the synthetic Greenland $d^{18}O$ reconstruction indicates the occurrence of millennial variability expressed by DO-like events (Barker et al., 2011).

Finally CT3, at 0.65 Ma, marks the end of the transition from the Lower and Mid-Pleistocene interval — characterized by 41-kyr–dominated cycles and smaller 23-kyr ones — to the Upper Pleistocene, with its 100-kyr–dominated cycles; see Fig. 2. The sawtooth pattern of the interglacial–glacial cycles is well established during this final interval, in contradistinction with the previous, more smoothly shaped pattern that appears to follow the obliquity variations. The global ice volume is maximal, exceeding the values observed earlier in the record, especially due to the larger contribution of the Northern American ice sheets. The latter now have a bigger impact on Northern Hemisphere climate than the Eurasian ice sheets (Batchelor et al., 2019). The IRD event intensity and frequency of occurrence increase (McManus et al., 1999) as well (Suppl. Fig. 3), leading to the major iceberg discharges into the North Atlantic named Heinrich events (HEs); see Heinrich (1988), Bond et al. (1992, 1993), and Obrochta et al. (2014). The interval of 1 Ma – about 0.4 Ma (CT4) is also the interval during which Northern Hemisphere ice sheets reached their southernmost extent (Batchelor et al., 2019). Applying Mg/Ca transfer functions, Elderfield et al. (2012) have estimated that the past 0.4 Myr water temperatures have been the highest the past 1.2 Myr, supporting the local temperature variations deduced from the Antarctic ice cores (Jouzel et al., 2007).

Supplementary Figures

Figure S1: KS test and Recurrence Quantitative Analysis (RQA) of CENOGRID benthic $\delta^{13}C$. a) KS test identifying abrupt transitions towards warmer conditions in red and cooler or colder conditions in blue; b) Recurrence plot (RP), and c) Recurrence rate (RR). The pink crosses and vertical green lines indicate the abrupt transitions (Table) detected by the RQA.

Figure S2: RQA of U1308 benthic $\delta^{13}C$. a) Time series in Ma; b) RP; and c) RR. Crosses similar than Fig. S1.

Figure S3: RQA of U1308 bulk carbonate $\delta^{18}0$. A) Time series in Ma of booth benthic $\delta^{18}O$ in blue and $\delta^{18}O$ bulk carbonate in green; b) RR; and c) RR). The pink crosses and vertical lines indicate the abrupt transitions (Table) detected by the RQA.

Fig. Supp.1

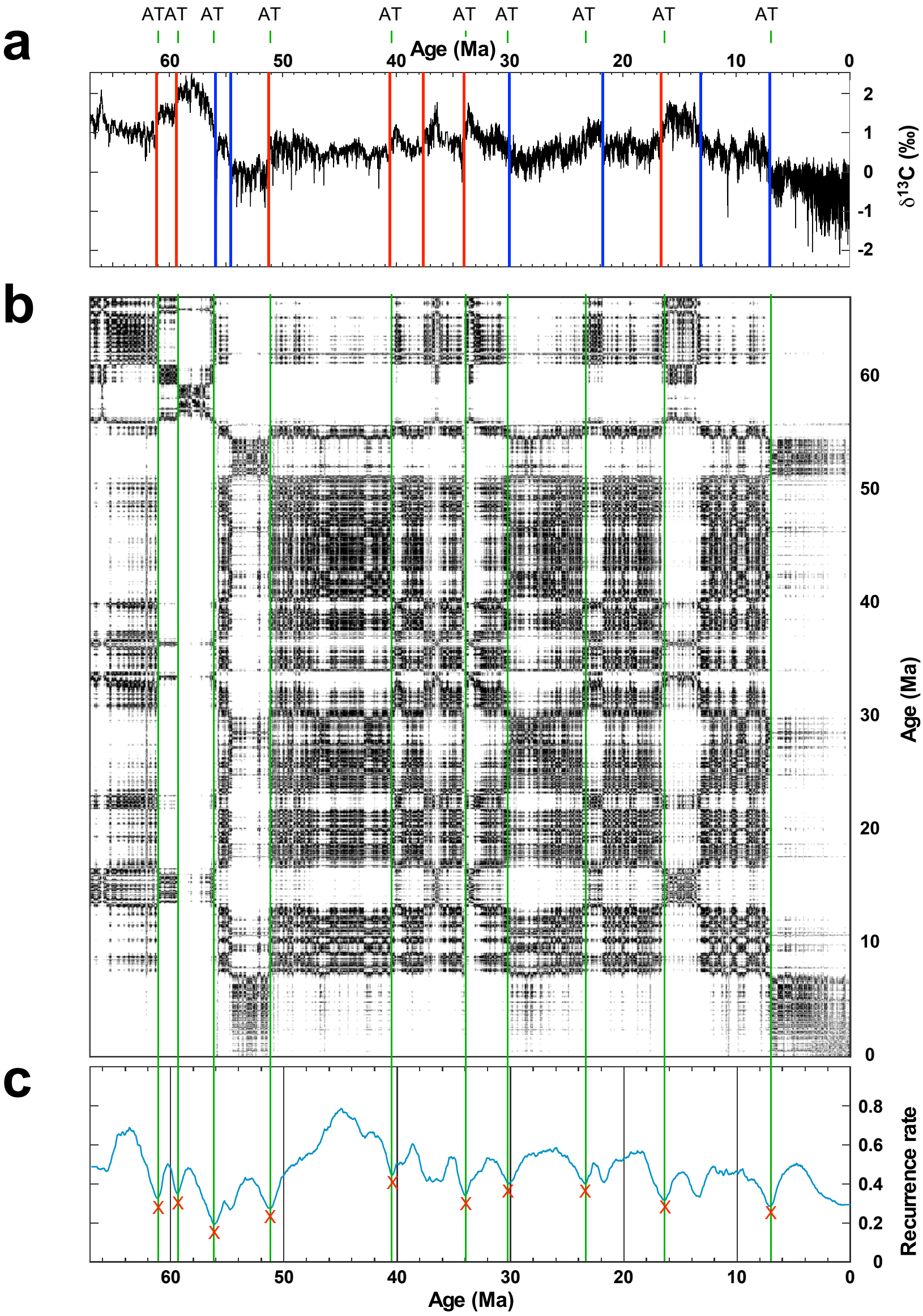
a
ATAT AT AT AT AT AT AT AT AT
Age (Ma)
60 50 40 30 20 10 0
2 1 0 -1 -2
δ13C (‰)
b
60 50 40 30 20 10 0
Age (Ma)
c
0.8 0.6 0.4 0.2 0
Recurrence rate
60 50 40 30 20 10 0
Age (Ma)

Supp. FIg2

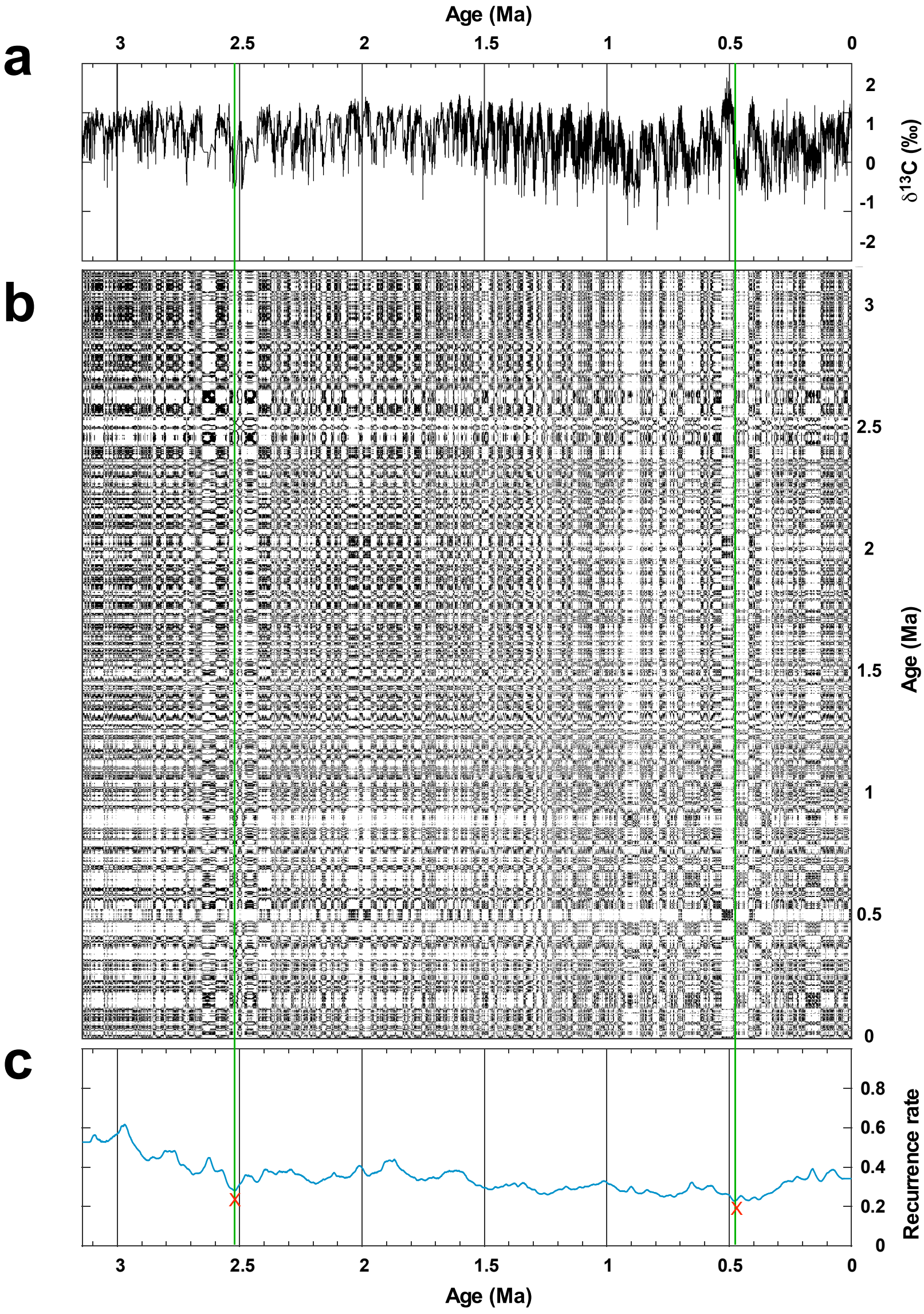
a
b
c
Age (Ma)
3
2.5
2
1.5
1
0.5
0
2
1
0
-1
-2
δ13C (‰)
3
2.5
2
1.5
1
0.5
0
Age (Ma)
0.8
0.6
0.4
0.2
0
Recurrence rate
3
2.5
2
1.5
1
0.5
0
Age (Ma)

Suppl. Fig. 3

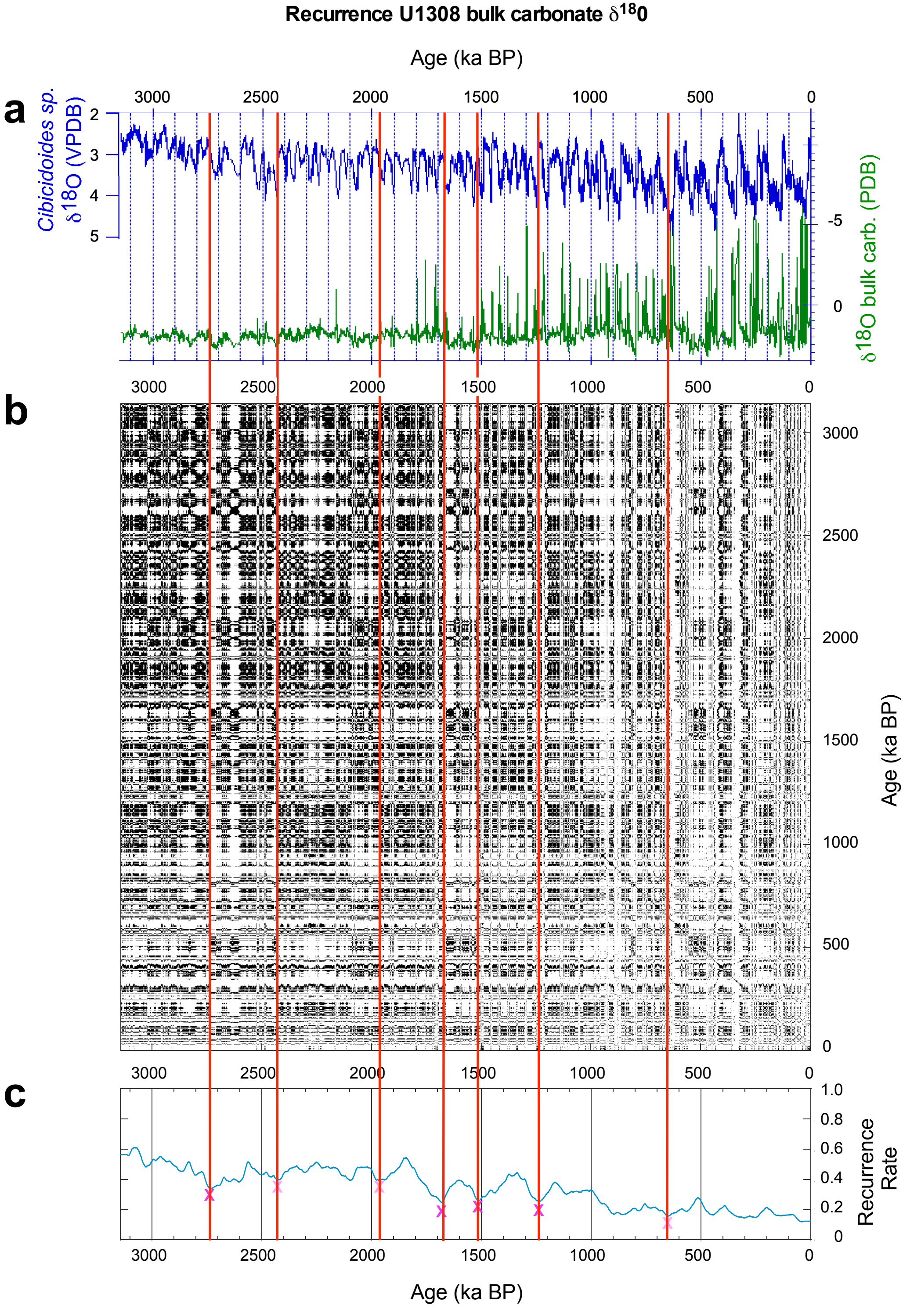
Recurrence U1308 bulk carbonate δ18O
Age (ka BP)
a
Cibicidoides sp. δ18O (VPDB)
δ18O bulk carb. (PDB)
b
Age (ka BP)
c
Recurrence Rate
Age (ka BP)

Supplementary Tables

Table S1: Recurrence Quantitative Analyses (RQA) of CENOGRID benthic $\delta^{18}0$ and $\delta^{13}C$, and U1308 benthic $\delta^{18}0$, $\delta^{13}C$, and bulk carbonate $\delta^{18}0$. For each parameters are listed 1st the age of the Abrupt transitions, the RR prominence value used to select the abrupt transition by comparison with the standard deviation, and 3d the significance with X above the RR prominence sd and $ very close to the sd. Ages are in Ma for the CENOGRID and in ka BP for the U1308 records respectively

Table S2: Statistics of the 66-34 Ma and 34 Ma-present for from top to bottom: the Global Mean sea level (GMSL) in meters from Miller et al. (2020), the CO2 concentration in PPMV from Beerling and Royer (2011), and for the CCD depth in meters from Pälike et al. (2012).

Table S3: Summary of the GMSL, CCD and CO2 concentration trends at the identified abrupt transitions TP1 to TP10.

Suppl. Tab. 1

CENOGRID δ18O, window: 1-6 Ma			CENOGRID δ13C, window: 1-6 Ma			U1308 δ18O, window: 60-250 ka			U1308 δ13C, window: 60-250 ka			U1308 bulk carbonate δ18O, window: 60-250 ka		
Ma BP	RR prominen	Significance	Ma BP	RR prominen	Significance	ka BP	RR prominen	Significance	ka BP	RR prominen	Significance	ka BP	RR prominen	Significance
33,85	0,41570578	X	56,15	0,49582588	X	2524	0,23796191	X	477	0,16393608	X	2732	0,20363551	X
47	0,33114787	X	34	0,24468463	X	1510	0,14169216	X	2521	0,15914759	X	1681	0,19748231	X
14,05	0,31556165	X	7,15	0,21940684	X	354	0,1239728	X	-	-		1510	0,13491356	X
62,65	0,23176521	X	61,15	0,17631944	X	614	0,11154923	X	-	-		1234	0,12752732	X
39,85	0,18154617	X	16,4	0,17583585	X	1248	0,08692142	X	-	-		1966	0,12498718	$
56,05	0,17128033	X	23,4	0,16939465	X	2925	0,07068202	$	-	-		653	0,12224033	$
58,05	0,12919749	X	40,45	0,16112753	X	-	-		-	-		2421	0,11758806	$
9,7	0,0862254	$	51,2	0,15785367	X	-	-		-	-		-	-	
-	-		59,4	0,13334579	X	-	-		-	-		-	-	
-	-		30,2	0,13193157	X	-	-		-	-		-	-	

Suppl. Tab2

Miller et al. (2020)	Age_cal Ma BP	Sea level (m)		Age_cal Ma BP	Sea level (m)
Minimum	0,98	-33,00		33,68	-1,90
Maximum	33,66	33,20		64,82	77,30
Points	1635,00	1635,00		1558,00	1558,00
Mean	17,32	-3,49		49,25	38,47
Median	17,32	-3,80		49,25	36,00
Std Deviation	9,44	12,90		9,00	14,85

Beerling & Royer (2011)	Age (Ma)	CO2 (ppm)		Age (Ma)	CO2 (ppm)
Minimum	0,00	80,00		34,00	100,00
Maximum	33,60	1232,00		65,00	1868,00
Points	289,00	289,00		81,00	77,00
Mean	14,29	329,81		49,17	626,96
Median	14,10	271,00		54,00	574,00
Std Deviation	8,39	164,47		9,73	311,79

Pälike et al. (2012)	Age (Ma)	eq CCD (m)		Age (Ma)	eq CCD (m)
Minimum	0,00	4100,00		33,75	2800,00
Maximum	33,50	4900,00		52,25	4300,00
Points	135,00	135,00		75,00	75,00
Mean	16,75	4586,30		43,00	3518,67
Median	16,75	4600,00		43,00	3500,00
Std Deviation	9,78	153,01		5,45	408,92

Suppl. Tab. 3

	TP1	TP2	TP3	TP4	TP5	TP6	TP7	TP8	TP9	TP10
GMSL	↘	↗	↘	↘	↗	⇘	↘	↘	↘	↘
CCD	-	-	-	↘	↗	⇘	↘	↘	↘	↘
CO_2	↗	↗	↗	↘	↘	⇘	↘	↘	↘	?

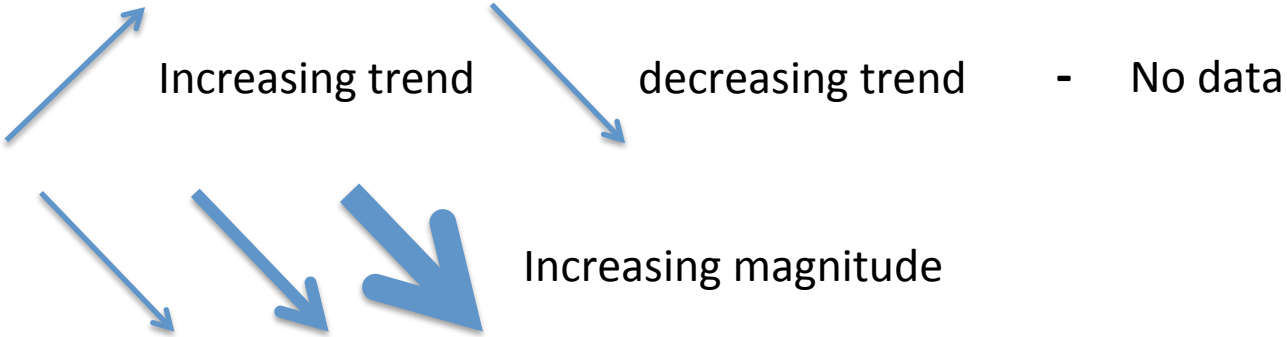

Supplementary references

Bailey, I., Hole, G., Foster, G., Wilson, P., Storey, C., Trueman, C., and Raymo, M.: An alternative suggestion for the Pliocene onset of major northern hemisphere glaciation based on the geochemical provenance of North Atlantic Ocean ice-rafted debris, Quat. Sci. Rev., 75, 181–194, https://doi.org/10.1016/j.quascirev.2013.06.004, 2013.

Barker, S., Knorr, G., Edwards, R. L., Parrenin, F., Putnam, A. E., Skinner, L. C., Wolff, E., and Ziegler, M.: 800,000 Years of Abrupt Climate Variability, Science, 334, 347–351, https://doi.org/10.1126/science.1203580, 2011.

Batchelor, C. L., Margold, M., Krapp, M., Murton, D., Dalton, A. S., Gibbard, P. L., Stokes, C. R., Murton, J. B., and Manica, A.: The configuration of Northern Hemisphere ice sheets through the Quaternary, Nat. Commun., 10, https://doi.org/10.1038/s41467-019-11601-2, 2019.

Beerling, D. and Royer, D.: Convergent Cenozoic CO2 history, Nat. Geosci., 4, 418–420, https://doi.org/10.1038/ngeo1186, 2011.

Berends, C. J., de Boer, B., and van de Wal, R. S. W.: Reconstructing the evolution of ice sheets, sea level, and atmospheric CO2 during the past 3.6 million years, Clim. Past, 17, 361–377, https://doi.org/10.5194/cp-17-361-2021, 2021.

Bond, G., Heinrich, H., Broecker, W., Labeyrie, L., McManus, J., Andrews, J., Huon, S., Jantschik, R., Clasen, S., Simet, C., Tedesco, K., Klas, M., Bonani, G., and Ivy, S.: Evidence for massive discharges of icebergs into the North Atlantic Ocean during the last glacial period., Nature, 360, 245–249, 1992.

Bond, G., Broecker, W., Johnsen, S., McManus, J., Labeyrie, L., Jouzel, J., and Bonani, G.: Correlations between climate records from North Atlantic sediments and Greenland ice., Nature, 365, 143–147, 1993.

Boulila, S., Galbrun, B., Miller, K., Pekar, S., Browning, J., Laskar, J., and Wright, J.: On the origin of Cenozoic and Mesozoic "third-order" eustatic sequences, Earth-Sci. Rev., 109, 94–112, https://doi.org/10.1016/j.earscirev.2011.09.003, 2011.

Broecker, W. S. and van Donk, J.: Insolation changes, ice volumes, and 0-18 record in deep-sea cores, Rev. Geophys. Space Phys., 8, 169–198, https://doi.org/10.1029/RG008i001p00169, 1970.

DeConto, R., Pollard, D., Wilson, P., Palike, H., Lear, C., and Pagani, M.: Thresholds for Cenozoic bipolar glaciation, Nature, 455, 652-U52, https://doi.org/10.1038/nature07337, 2008.

Elderfield, H., Ferretti, P., Greaves, M., Crowhurst, S., McCave, I. N., Hodell, D., and Piotrowski, A. M.: Evolution of Ocean Temperature and Ice Volume Through the Mid-Pleistocene Climate Transition, Science, 337, 704–709, https://doi.org/10.1126/science.1221294, 2012.

Heinrich, H.: Origin and Consequences of Cyclic Ice Rafting in the Northeast Atlantic Ocean during the Past 130,000 years, Quat. Res., 29, 142–152, 1988.

Hodell, D. A. and Channell, J. E. T.: Mode transitions in Northern Hemisphere glaciation: co-evolution of millennial and orbital variability in Quaternary climate, Clim. Past, 12, 1805–1828, https://doi.org/10.5194/cp-12-1805-2016, 2016.

Houben, A., van Mourik, C., Montanari, A., Coccioni, R., and Brinkhuis, H.: The Eocene-Oligocene transition: Changes in sea level, temperature or both?, Palaeoclimatol. Palaeoecol. Palaeogeogr., 335, 75–83, https://doi.org/10.1016/j.palaeo.2011.04.008, 2012.

Jakob, K. A., Wilson, P. A., Pross, J., Ezard, T. H. G., Fiebig, J., Repschlager, J., and Friedrich, O.: A new sea-level record for the Neogene/Quaternary boundary reveals transition to a more stable East Antarctic Ice Sheet, Proc. Natl. Acad. Sci. U. S. A., 117, 30980–30987, https://doi.org/10.1073/pnas.2004209117, 2020.

Jouzel, J., Masson-Delmotte, V., Cattani, O., Dreyfus, G., Falourd, S., Hoffmann, G., Minster, B., Nouet, J., Barnola, J.,

Chappellaz, J., Fischer, H., Gallet, J., Johnsen, S., Leuenberger, M., Loulergue, L., Luethi, D., Oerter, H., Parrenin, F., Raisbeck, G., Raynaud, D., Schilt, A., Schwander, J., Selmo, E., Souchez, R., Spahni, R., Stauffer, B., Steffensen, J., Stenni, B., Stocker, T., Tison, J., Werner, M., and Wolff, E.: Orbital and millennial Antarctic climate variability over the past 800,000 years, Science, 317, 793–796, https://doi.org/10.1126/science.1141038, 2007.

Knudsen, M. F., Norgaard, J., Grischott, R., Kober, F., Egholm, D. L., Hansen, T. M., and Jansen, J. D.: New cosmogenic nuclide burial-dating model indicates onset of major glaciations in the Alps during Middle Pleistocene Transition, Earth Planet. Sci. Lett., 549, https://doi.org/10.1016/j.epsl.2020.116491, 2020.

McManus, J. F., Oppo, D. W., and Cullen, J. L.: A 0,5-million-year record of millennial-scale climate variability in the North Atlantic, Science, 283, 971–975, 1999.

Miller, K., Wright, J., and Fairbanks, R.: Unlocking the ice-house Oligocene-Miocene oxygen isotopes, eustasy, and margin erosion, J. Geophys. Res.-Solid Earth Planets, 96, 6829–6848, https://doi.org/10.1029/90JB02015, 1991.

Miller, K., Browning, J., Schmelz, W., Kopp, R., Mountain, G., and Wright, J.: Cenozoic sea-level and cryospheric evolution from deep-sea geochemical and continental margin records, Sci. Adv., 6, https://doi.org/10.1126/sciadv.aaz1346, 2020.

Muttoni, G., Carcano, C., Garzanti, E., Ghielmi, M., Piccin, A., Pini, R., Rogledi, S., and Sciunnach, D.: Onset of major Pleistocene glaciations in the Alps, Geology, 31, 989–992, https://doi.org/10.1130/g19445.1, 2003.

Naafs, B. D. A., Hefter, J., and Stein, R.: Millennial-scale ice rafting events and Hudson Strait Heinrich(-like) Events during the late Pliocene and Pleistocene: a review, Quat. Sci. Rev., 80, 1–28, https://doi.org/10.1016/j.quascirev.2013.08.014, 2013.

Obrochta, S. P., Crowley, T. J., Channell, J. E. T., Hodell, D. A., Baker, P. A., Seki, A., and Yokoyama, Y.: Climate variability and ice-sheet dynamics during the last three glaciations, Earth Planet. Sci. Lett., 406, 198–212, https://doi.org/10.1016/j.epsl.2014.09.004, 2014.

Palike, H., Lyle, M., Nishi, H., Raffi, I., Ridgwell, A., Gamage, K., Klaus, A., Acton, G., Anderson, L., Backman, J., Baldauf, J., Beltran, C., Bohaty, S., Bown, P., Busch, W., Channell, J., Chun, C., Delaney, M., Dewangan, P., Dunkley Jones, T., Edgar, K., Evans, H., Fitch, P., Foster, G., Gussone, N., Hasegawa, H., Hathorne, E., Hayashi, H., Herrle, J., Holbourn, A., Hovan, S., Hyeong, K., Iijima, K., Ito, T., Kamikuri, S., Kimoto, K., Kuroda, J., Leon-Rodriguez, L., Malinverno, A., Moore, T., Murphy, B., Murphy, D., Nakamura, H., Ogane, K., Ohneiser, C., Richter, C., Robinson, R., Rohling, E., Romero, O., Sawada, K., Scher, H., Schneider, L., Sluijs, A., Takata, H., Tian, J., Tsujimoto, A., Wade, B., Westerhold, T., Wilkens, R., Williams, T., Wilson, P., Yamamoto, Y., Yamamoto, S., Yamazaki, T., and Zeebe, R.: A Cenozoic record of the equatorial Pacific carbonate compensation depth, Nature, 488, 609-+, https://doi.org/10.1038/nature11360, 2012.

Paxman, G., Jamieson, S., Hochmuth, K., Gohl, K., Bentley, M., Leitchenkov, G., and Ferraccioli, F.: Reconstructions of Antarctic topography since the Eocene-Oligocene boundary, Palaeoclimatol. Palaeoecol. Palaeogeogr., 535, https://doi.org/10.1016/j.palaeo.2019.109346, 2019.

Pollard, D. and DeConto, R.: Continuous simulations over the last 40 million years with a coupled Antarctic ice sheet-sediment model, Palaeoclimatol. Palaeoecol. Palaeogeogr., 537, https://doi.org/10.1016/j.palaeo.2019.109374, 2020.

Rohling, E., Yu, J., Heslop, D., Foster, G., Opdyke, B., and Roberts, A.: Sea level and deep-sea temperature reconstructions suggest quasi-stable states and critical transitions over the past 40 million years, Sci. Adv., 7, https://doi.org/10.1126/sciadv.abf5326, 2021.

Rousseau, D., Bagniewski, W., and Ghil, M.: Abrupt climate changes and the astronomical theory: are they related?, Clim. Past, 18, 249–271, https://doi.org/10.5194/cp-18-249-2022, 2022.

Smith, Y., Hill, D., Dolan, A., Haywood, A., Dowsett, H., and Risebrobakken, B.: Icebergs in the Nordic Seas Throughout the Late Pliocene, Paleoceanogr. PALEOCLIMATOLOGY, 33, 318–335,

https://doi.org/10.1002/2017PA003240, 2018.

van de Wal, R. S. W., de Boer, B., Lourens, L. J., Koehler, P., and Bintanja, R.: Reconstruction of a continuous high-resolution CO2 record over the past 20 million years, Clim. Past, 7, 1459–1469, https://doi.org/10.5194/cp-7-1459-2011, 2011.